NASA-CR- 174924

NASA Contractor Report 174924

NASA-CR-174924
19860002007

LATERAL DAMPERS FOR THRUST BEARINGS

Final Report

D.H. Hibner and D.R. Szafir

NASA

NF01219

400 Main Street
East Hartford Connecticut 06108

In reply please refer to:
DHH:dla:0243k - MS 163-09
Ref. No. PWA-5966-17

October 17, 1985

To: National Aeronautics and Space Administration
             Lewis Research Center
             21000 Brookpark Road
             Cleveland, Ohio 44135

Attention: Dr. David Fleming, M.S. 23-3

Subject: Lateral Dampers for Thrust Bearings Program Final Report

Reference: NASA Contract NAS3-23932

Enclosures: One 'Camera Ready' Copy plus twenty copies of Subject Report,
             PWA-5966-17

Gentlemen:

The enclosed copies of the subject report are submitted in compliance with the
terms of the referenced contract.

Sincerely yours,

UNITED TECHNOLOGIES CORPORATION
Pratt & Whitney Group
Engineering Division

D. H. Hibner
Program Manager

N86-11474#

1.REPORT NO. NASA CR-174924	2. GOVERNMENT AGENCY	3.RECIPIENT'S CATALOG NO.	
4.TITLE AND SUBTITLE LATERAL DAMPERS FOR THRUST BEARINGS		5. REPORT DATE August 1985	
		6. PERFORMING ORG. CODE	
7.AUTHOR(S) D. H. Hibner and D. R. Szafir		8. PERFORMING ORG. REPT. NO. PWA-5966-17	
9.PERFORMING ORG. NAME AND ADDRESS UNITED TECHNOLOGIES CORPORATION Pratt & Whitney Engineering Division		10. WORK UNIT NO.	
		11. CONTRACT OR GRANT NO. NAS3-23932	
12. SPONSORING AGENCY NAME AND ADDRESS National Aeronautics and Space Administration Washington, D.C. 20546		13. TYPE REPT./PERIOD COVERED Final Report	
		14. SPONSORING AGENCY CODE	

15. SUPPLEMENTARY NOTES

16. ABSTRACT

This program focused on the development of lateral damping schemes for thrust bearings, ranking their applicability to various engine classes, selecting the best concept for each engine class and performing an in-depth evaluation. Five major engine classes were considered: large transport, military, small general aviation, turboshaft, and non-manrated. Damper concepts developed for evaluation were: curved beam, constrained and unconstrained elastomer, hybrid boost bearing, hydraulic thrust piston, conical squeeze film, and rolling element thrust face.

17. KEY WORDS (SUGGESTED BY AUTHOR(S)) Rotor Dynamics, Thrust Bearings, Lateral Dampers, Gas Turbine Engines, Squeeze Film Dampers, Elastomer Dampers		18. DISTRIBUTION STATEMENT Unclassified - Unlimited		
19. SECURITY CLASS THIS (REPT) Unclassified	20. SECURITY CLASS THIS (PAGE) Unclassified		21. NO. PGS 77	22. PRICE *

FOREWORD

This report documents the results of a study of lateral dampers for thrust bearings. The study was conducted for the National Aeronautics and Space Administration (NASA) under Contract NAS3-23932.

The NASA Project Manager for this study was Dr. David P. Fleming, Lewis Research Center, Cleveland, Ohio, and the Pratt & Whitney Program Manager was David H. Hibner. Major technical contributors were Dennis F. Buono, Gabriel L. Suciu, and David R. Szafir.

Table of Contents

Table of Contents (continued)

Table of Contents (continued)

List of Figures

List of Figures

List of Tables

SECTION 1.0

SUMMARY

This program focused on the development of lateral damping schemes for thrust bearings, ranking their applicability to various engine classes, and selecting/evaluating the best concept for each engine class. Five major engine classes were considered: large transport, military, small general aviation, turboshaft, and non-manrated. Damper concepts developed for evaluation were: curved beam, constrained and unconstrained elastomer, hybrid boost bearing, hydraulic thrust piston, conical squeeze film, and rolling element thrust face.

Damper concepts were evaluated using nine assessment parameters: effectiveness, size, cost, thrust capability, durability, design flexibility, installation, weight, and risk. Each was assigned a numerical value which ranked its respective applicability. The ranking was done on a basis of 1 to 5 in order of increasing goodness. Based on the ranking concepts for each engine type and establishment of weighting factors, damper selection was determined for each engine type, as follows:

o   The curved beam damper had the highest rating for the large transport and military engine classification.

o   The elastomer was found best for the small general aviation and non-manrated engines.

o   The conical squeeze film rated best for the turboshaft engine.

Due to the multiple selection of the curved beam and elastomer dampers, the in-depth analysis of the concepts was limited to three engine classifications: large transport, turboshaft, and small general aviation.

A hypothetical, representative engine model was specified for each of the engine classes. The chosen damper concepts were then geometrically perturbated in order to assess their ability to meet sensitivity requirements within confines of the compartment size and environment. Results of the analysis showed that each damper could meet normal and high load imbalance; however, due to the novel nature of the designs, each has a certain degree of risk associated with it.

SECTION 2.0

INTRODUCTION

Current and advanced gas turbine engines have a recognized need for active vibration control. Higher speeds and more flexible rotor designs result in sensitive rotor vibration modes in the engine operating range. Optimum performance and long life durability goals require that vibration amplitudes and loads be minimized.

Squeeze film dampers have successfully met engine requirements in the past, but advanced engine designs impose an additional requirement that dampers be used at thrust bearing locations. Conventional squeeze film dampers cannot support thrust loads without the complexity of an additional thrust structure or the nonlinearity of friction forces at rubbing thrust surfaces. As a result, improved damper concepts are required for satisfactory application to thrust bearings in advanced gas turbine engines.

This program was designed to add to the technology base which will be used to develop dampers for modern gas turbine engines which require dampers at thrust bearing locations. The dynamic characteristics of five major classes of modern jet engines were defined and damping systems were developed to react thrust and control engine vibration response under low and high imbalance loads.

Section 3.0, "Damper Concepts and Application Requirements," discloses the various damper concepts developed in this study as well as defining the constraints which the dampers need to meet for the various engine classes.

Section 4.0, "Damper Concept Ranking," describes the ranking procedure and presents the results of the ranking for the various engine types.

Section 5.0, "Analytical Methods and Evaluation," describes the analytical methods used, in terms of damper concept equations for stiffness and damping, engine model development and mode selection. In addition, a detailed evaluation of the selected dampers is presented for the particular engines.

Section 6.0, "Conclusions and Recommendations," presents the results of this study and recommendations for additional efforts needed to define applicability of the selected damper concepts.

SECTION 3.0

DAMPER CONCEPTS AND APPLICATION REQUIREMENTS

3.1 Damper Concepts

The comparison of state-of-the-art thrust bearing damper technology to the stringent requirements of aggressive engine design indicates the need for innovative damper concepts. The basic problems with current designs are size, weight, and durability, and stem from the design approach that uses two separate components to carry thrust and supply damping. The proposed concepts combine the two functions into the same mechanism and therefore represent good approaches to solving the problem of providing adequate damping and thrust load capability.

A literature survey identified several candidate concepts. In addition, concepts were defined from variations of "standard" damper concepts and innovations derived from Pratt & Whitney design experience.

The major conclusion drawn from the literature survey is that there were no damper concepts in the literature that could carry thrust loads without either a thrust washer friction face or a mechanical spring structure in parallel with the damper. One possible exception is the elastomer damper, which can carry a very light thrust load in shear or could have a thrust "cushion" on an axial face to carry the load. Although there were thrust support concepts in the literature, they were not necessarily presented in connection with a damper. These concepts were combined with conventional dampers to provide complete packages. A brief description of each concept is provided in the following sections.

3.1.1 Curved Beam Damper

The curved beam damper, shown in Figure 1, has been demonstrated to be a good damper approach for large and small jet engines (References 1 through 3). The damper contains circumferential curved springs or beams which center the damper, provide radial stiffness, and maintain pockets of oil which are squeezed under load. The radial stiffness depends on the beam geometry and end conditions and is independent of oil film behavior if cavitation is prohibited. Damping is provided by pumping oil through the inlet ports as the damper whirls. Proper specification of the damper clearance, supply pressure and orifice geometry will provide constant stiffness and damping coefficients over a large amplitude range making this a linear element.

Thrust loads can be easily supported by the curved beam damper with very little change to the design. The curved beams are supported on the inside and outside by a series of short axial rails or feet arranged in a staggered pattern. If thrust is applied at the ends of the rails at the beam inner diameter and reacted at the ends of the rails at the beam outer diameter, then the thrust load will be carried without interfering with radial motion. This is a very efficient structure for carrying load in the axial direction because the large dimension in that direction results in low bending stress.
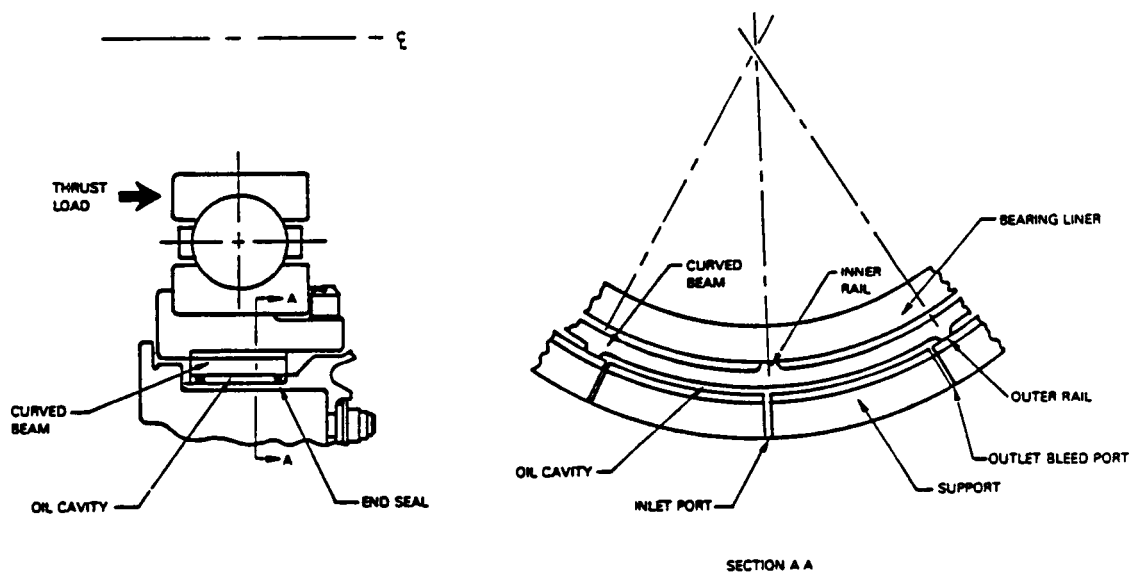
Figure 1   Curved Beam Damper

3.1.2 Conical Squeeze Film

The conical squeeze film configuration, Figure 2, is a variation of the hydraulic thrust piston (described in Section 3.1.6). The approach uses a conventional sealed-squeeze film with an inclined oil film to give a projected axial area which can provide thrust capability. The inclined damper will have reduced effectiveness which can be recovered by decreasing clearance as cone angle goes up. Since damper performance (i.e., stiffness and damping) is a function of clearance and supply pressure, the damper behavior will be affected by thrust load.
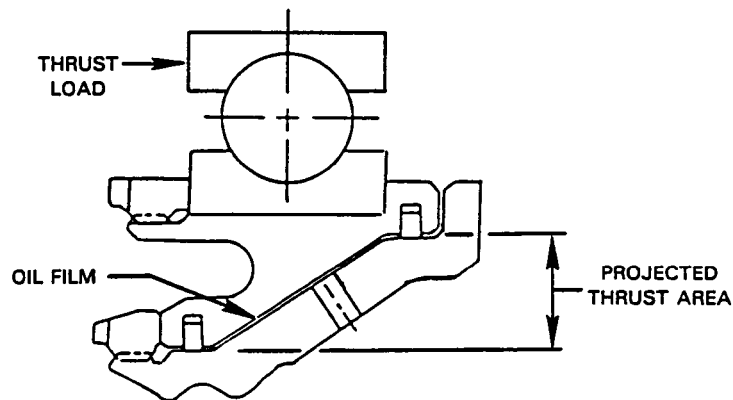
Figure 2   Conical Squeeze Film

4

3.1.3 Conical Elastomer Damper

Elastomeric dampers are an alternative to squeeze film dampers that offer the advantages of compactness, self-sufficiency (no oil supply), low cost, and a wide range of stiffness and damping characteristics. Design limitations exist due to material property degradation at elevated temperatures of 300°F to 500°F and in hostile oil environments, but improved cooling and packaging (i.e., shielding from oil) can overcome these problems. Anticipated improvements in materials may overcome property degradation problems. Research conducted by Pratt & Whitney and others (Reference 12) has demonstrated the effectiveness of elastomers and elastomeric dampers and has established analytical and design guidelines.

Elastomers can support load in both shear and compression and will dissipate energy when cyclically loaded. A conical elastomer (Figure 3) can carry both thrust and radial loads, but damper effectiveness will be compromised as thrust requirements and cone angle increase. The conical elastomer damper has an advantage over the conical squeeze film in that the elastomer has significant load/damping capacity in shear and therefore can tolerate higher cone angles.
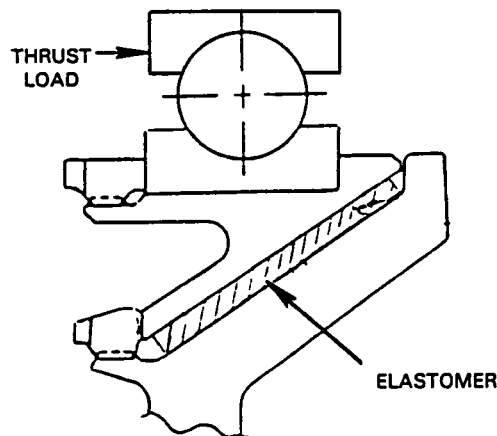
Figure 3   Conical Elastomer Damper

3.1.4 Constrained Elastomeric Damper

An elastomeric damper may have a significant drawback when applied as a thrust bearing damper, particularly under high thrust conditions. Axial flexibility must be limited in most applications. Axial motion may cause blade and stator interaction or may make it difficult to control tip gaps in angled compressor or turbine stages. In addition, power takeoff gears on the engine main shafts cannot tolerate excessive looseness or tightness that would occur if axial shaft motion were permitted.

A constrained elastometric damper, as shown in Figure 4, can overcome the problems associated with axial flexibility. In this design, a metal enclosure around the elastomer is configured to allow radial flexibility and compression of the elastomer for damping. The thrust load would be carried by the metal enclosure, which could be designed to have sufficient axial stiffness without radial stiffness by maintaining a small radial height. This approach introduces a cyclically loaded structural member which may be necessary if axial motion is a problem.
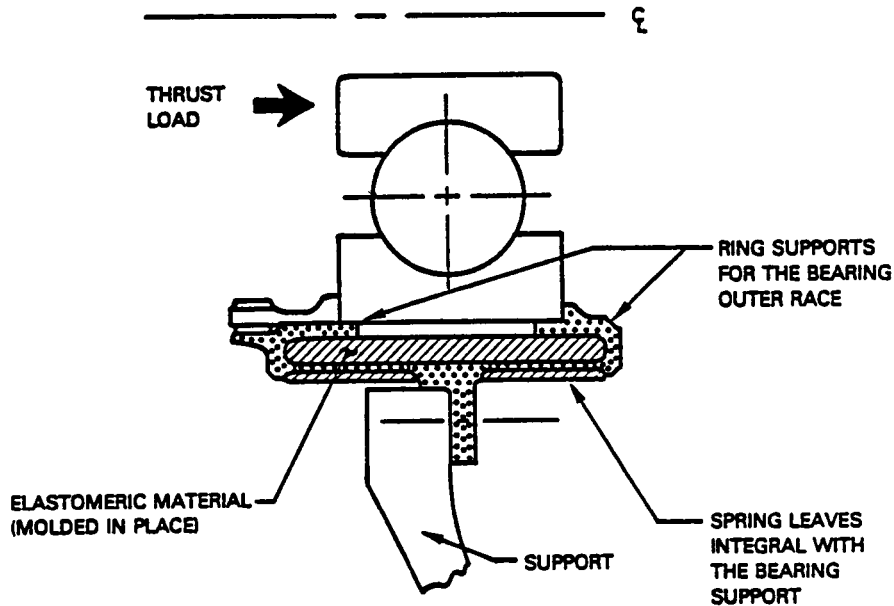
Figure 4   Constrained Elastomeric Damper

3.1.5 Hybrid Boost Bearing

The hybrid boost bearing concept (Figure 5), which was developed and studied in 1969 by Wilcock and Winn (Reference 11), comprises a fluid film thrust bearing and angular contact ball bearing in parallel to carry thrust. The fluid film thrust bearing could be either hydrostatic or hydrodynamic and is employed to reduce the loading on the ball bearing, thereby increasing life. With the reduced thrust on the ball bearing, an oil film can be included between the bearing outer race and housing, and damping is accomplished as in conventional squeeze film dampers. An advantage of this concept is the reduced load on the bearing, but a drawback is the potentially high oil flows required.
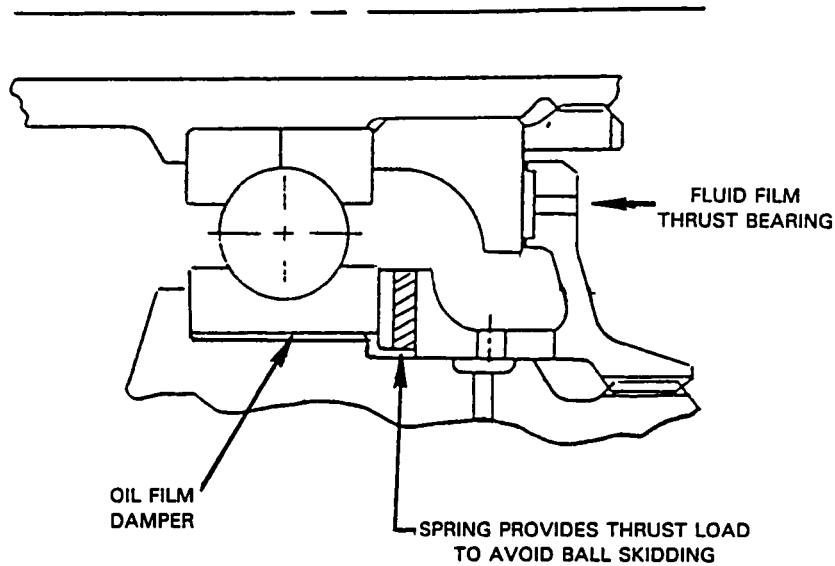
Figure 5   Hybrid Boost Bearing

3.1.6 Hydraulic Thrust Piston

The hydraulic thrust piston approach, Figure 6, utilizes an annular hydraulic piston attached to the thrust side of a conventional squeeze film damper to carry the thrust load. The piston is supported by pressurized oil from the engine oil system, and thrust capacity is therefore determined by available oil pressure and piston size. Modulation of oil pressure could be used to vary thrust capacity for different operating conditions. This concept has the advantage of compactness and minimum risk due to its simplicity.
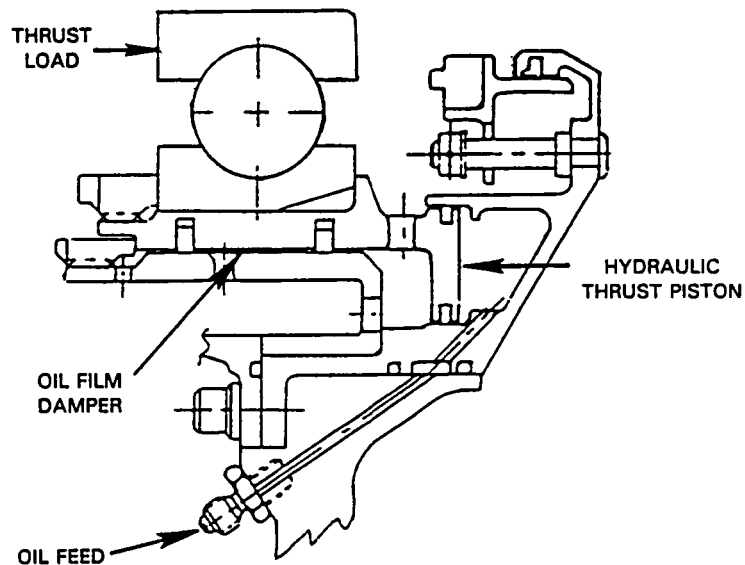
Figure 6   Hydraulic Thrust Piston

7

3.1.7 Rolling Element Thrust Face

The rolling element thrust face approach, Figure 7, is similar to the friction face thrust washer type of thrust support except that the friction forces are greatly reduced by the rolling contact elements. As shown in Figure 7, spherical rolling elements carry thrust and a leaf spring dissipates energy via friction. The two function independently and the rolling element could be used with a squeeze film or elastomer damper. The rolling elements need not be spherical but could be "aspirin" shaped with larger radius spherical end surfaces to reduce contact stress. This is possible due to limited radial excursions expected in most applications.
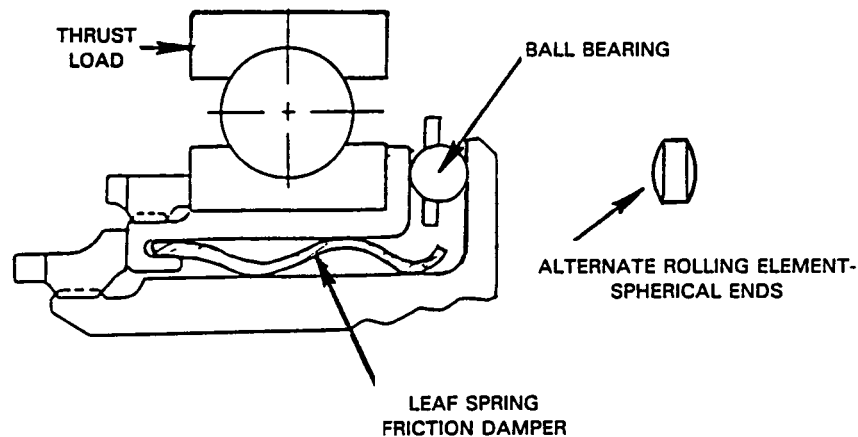
Figure 7   Rolling Element Thrust Face

3.2 Damper Application Requirements

A survey was conducted of all Pratt & Whitney engine design experience to define the general requirements for the thrust bearing dampers. The range of applications covered five engine classes spanning the application range from 50 lb. thrust non-manrated engines to 60,000 lb. thrust large transport engines plus turboshaft engines. Some of the engine classes include multispool engines, but only high spool shafts are considered because they have greatest need for thrust bearing dampers.

Table I summarizes the major damper requirements for the five engine classes, i.e., large transport, military, small general aviation, turboshaft, and non-manrated. The important parameters include speed, load, size, stiffness, and damping, as well as an indication of life requirements and temperature environment. The first observation from this table is that each class covers a broad range and there is substantial overlap between classes. The greatest distinctions between classes are the thrust load requirement and size constraints.

8

Table I

Damper Application Requirements

	Large Transport	Military	Small General Aviation	Turboshaft	Non-Manrated
RPM	7,000-15,000	10,000-15,000	20,000-45,000	20,000-50,000	50,000-100,000
Thrust	71,000-267,000 N 16,000- 60,000 lb	53,500-110,000 N 12,000-25,000 lb	4,500-15,500 N 1,000-3,500 lb	370-11,000 kW 500-15,000 shp	200-9,000 N 50-2,000 lb
Radial Load - N - lb	1,800-9,000 400-2,000	1,300-3,600 300-800	200-900 50-200	200-4,500 50-1,000	90-450 20-100
Axial Load - N - lb	4,500-67,000 1,000-15,000	9,000-45,000 2,000-10,000	1,800-6,700 400-1,500	2,000-22,000 500-5,000	450-4,500 100-1,000
Radial Stiffness - MN/m - lb/in x 10^3	18-53 100-300	0-70 0-400	4-53 20-300	4-53 20-300	0-18 0-100
Damping - NS/m - lb-sec/in	52,500-193,000 300-1,100	12,300-158,000 70-900	0-131,500 0-750	0-131,500 0-750	0-17,500 0-100
Axial Play - cm - in	0-0.076 0-0.030	0-.076 0-.030	0-0.076 0-0.030	0-0.076 0-0.030	0-0.076 0-0.030
Temperature - °K - °F	395-450 250-350	365-420 200-300	365-590 200-600	365-590 200-600	365-590 200-600
Life - hrs	10,000-30,000	4,000-30,000	5,000-25,000	5,000-25,000	500+
Bearing O.D. - cm - in	15.2-33.0 6.0-13.0	12.7-19.0 5.0-7.5	5.1-10.2 2.0-4.0	5.1-15.2 2.0-6.0	2.5-7.6 1.0-3.0
Bearing Length - cm - in	2.5-7.6 1.0-3.0	2.5-7.6 1.0-3.0	1.5-3.8 0.6-1.5	1.5-3.8 0.6-1.5	1.3-2.5 0.5-1.0
Radial Height - cm Available - in	2.5-16.5 1.0-6.5	1.9-5.1 0.75-2.0	2.5-5.1 1.0-2.0	2.0-5.1 0.8-2.0	0.0-2.5 0.0-1.0

SECTION 4.0

DAMPER CONCEPT RANKING

4.1 Ranking Procedure

A ranking procedure was developed to assess the performance of the selected damper concepts for each engine type. This procedure is formulated to encompass various parameters needed to fully assess a damper.

4.1.1 Assessment Parameters

The nine parameters used to rank the applicability of each damper concept are defined as follows:

1. Damper Effectiveness - The ability of the damper to meet the required needs for lateral damping and stiffness as listed in Table I.

2. Size - The ability of the damper to meet the size requirements in terms of effective bearing outer diameter, length, and radial height available as listed in Table I.

3. Cost - Relative overall cost for material, fabrication and installation.

4. Thrust Capability - The ability of the damper to meet the axial play and load requirements listed in Table I.

5. Durability - The ability of the damper to meet the life and temperature requirements listed in Table I.

6. Design Flexibility - The ability to modify damper operating characteristics (i.e., stiffness and damping) without major redesign.

7. Installation - Simplicity of implementation and assembly.

8. Weight - Relative overall weight including support hardware.

9. Risk - Relative risk based on untried technology of the concept.

4.1.2 Ranking System

The assessment parameters for each damper concept were assigned a numerical rating indicating their ability to be met. The rating system is a five point system as follows:

$$
\begin{array}{rcl}
\text{Poor} &=& 1 \\
\text{Fair} &=& 2 \\
\text{Good} &=& 3 \\
\text{Very Good} &=& 4 \\
\text{Excellent} &=& 5
\end{array}
$$

Rating on a numerical basis allowed the means to apply weighting factors for damper concept comparison purposes.

10

4.2 Damper Concept Ranking

4.2.1 Curved Beam Damper (Figure 8)

Effectiveness: The design was shown to work most effectively under lower speed/higher diameter engines such as the large transport and military engines. The smaller engines require extremely high supply pressure (greater than 1000 psi) in order to suppress cavitation. Therefore, these engines were ranked lower due to this requirement.

Size: In order to meet dynamic requirements, large diameters are needed. Thus, smaller engines suffered on size rating.

Cost: Cost was judged to be moderate based on multi-ringed construction and machining required.

Thrust Capability: This concept rated very high due to bi-directional thrust capability plus the fact that the load is taken by a structural member.

Durability: Simplicity and lack of sealing requirements result in a high rating. Fatigue does not appear to be a problem.

Design Flexibility: Ring redesign via orifice diameter and thickness change offers good range for modification of dynamic characteristics.

Installation: Ring assembly and required plumbing rate this concept as moderately difficult.

Weight: Depending on required stiffness/damping, the large diameter requirement can add appreciable weight.

Risk: Based on simplistic design plus the ability to supply axial and lateral support with loss of oil supply, the concept is judged to have minimal risk.

Summary: Provided sufficient oil supply is available, as well as adequate diameter, the curved beam damper offers exceptional potential.
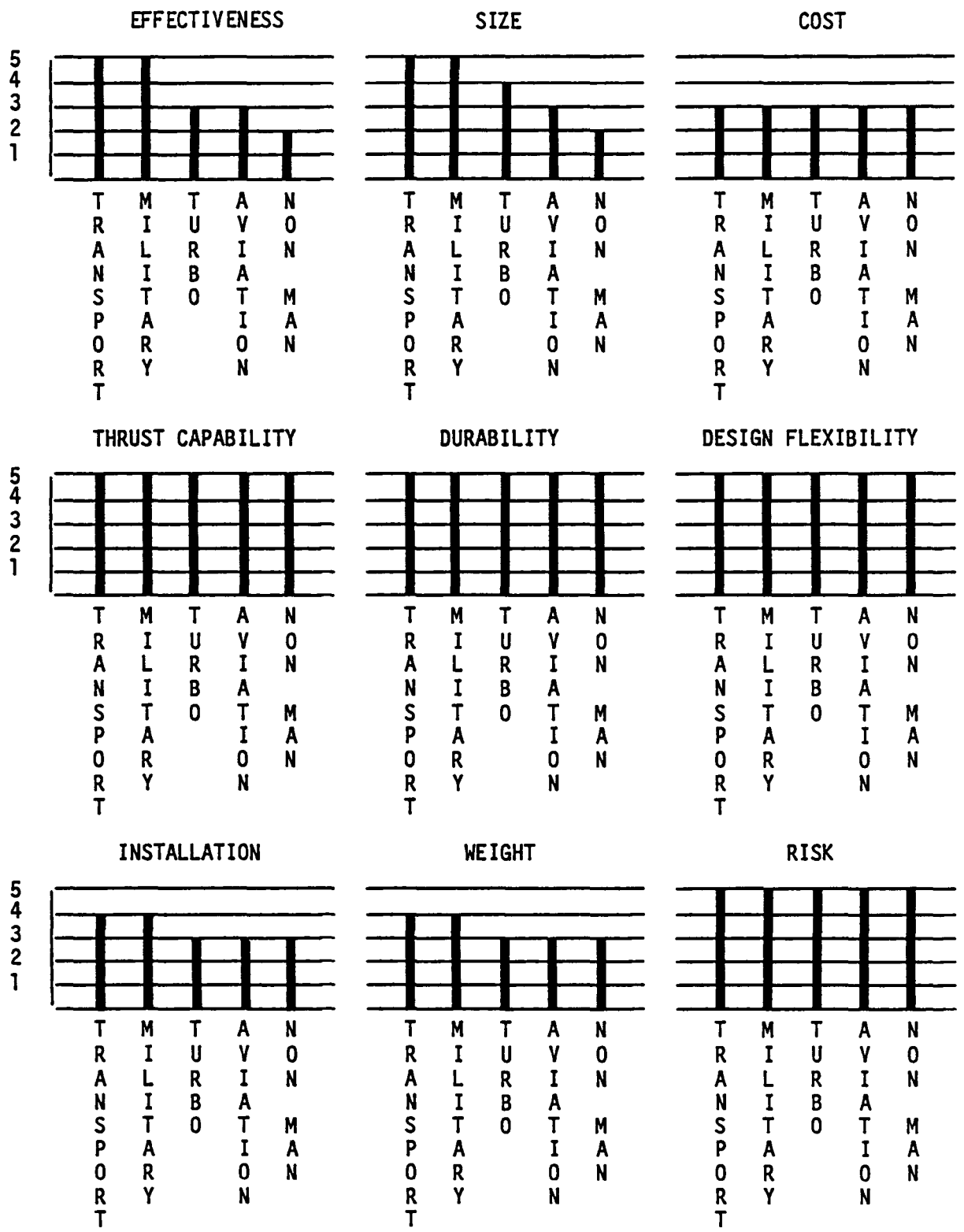
Figure 8   Curved Beam Damper Ranking

4.2.2 Conical Elastomer Damper (Figure 9)

Effectiveness:
: The stiffness and damping characteristics of elastomer dampers were the most difficult to assess. However, in general, it was resolved that elastomer use below 350°F was feasible. The smaller engines were downrated because the potentially higher temperature ranges would degrade the dynamic characteristics. In addition, axial preload can alter the required lateral characteristics.

Size:
: Relative size requirements were judged to be very good.

Cost:
: Cost was judged to be very good based on self-sufficiency of the concept, i.e., no lubrication required.

Thrust Capability:
: A serious problem with using an elastomer to take thrust is that axial straining of the elastomer can significantly alter the dynamic characteristics. In addition, sizing the elastomer to take axial load may affect attainment of required lateral stiffness and damping.

Durability:
: Based on a fair amount of testing by the industrial and research community, elastomers were judged to have good durability. Small engine types were given reduced ratings due to questionable durability associated with higher operating temperatures.

Design Flexibility:
: Rated very good overall based on simplicity of concept.

Installation:
: Rated excellent due to simplicity and lack of plumbing requirements.

Weight:
: Inherently excellent.

Risk:
: High risk associated with the use of elastomers. Substantial testing is needed to justify the design.

Summary:
: Elastomers are conceptually attractive. Their compactness, low cost and weight are difficult to overlook, provided sufficient development effort is expended.
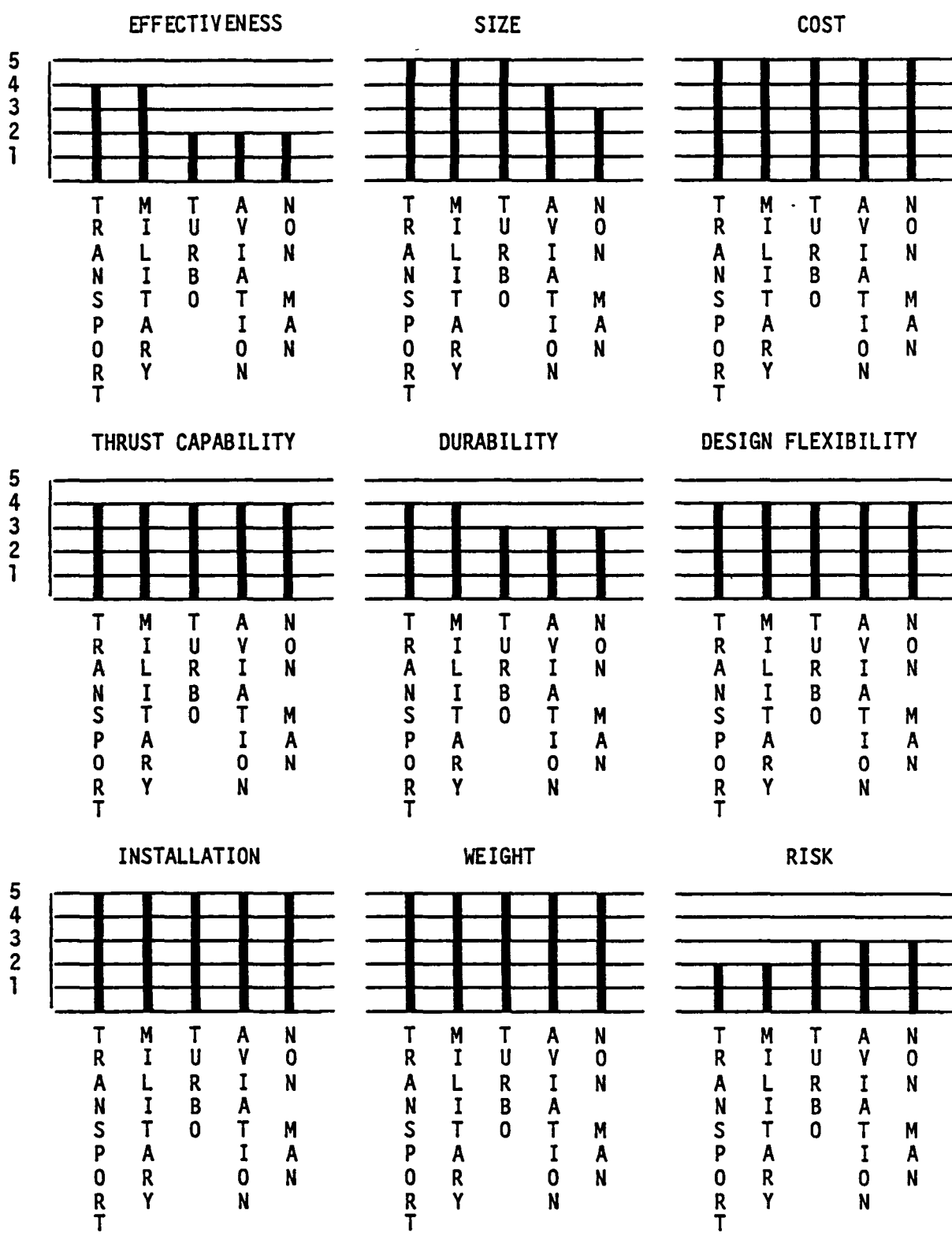
Figure 9   Conical Elastomer Damper Ranking

4.2.3 Constrained Elastomer Damper (Figure 10)

Effectiveness:
Same as the general elastomer, with the exception that the need of the elastomer to carry axial load is eliminated, resulting in more predictable characteristics.

Size:
Generally comparable to the elastomer.

Cost:
Increased cost due to thrust carrying ring and machining requirements.

Thrust Capability:
Excellent due to the structural member used to take bi-directional thrust load.

Durability:
Comparable to the elastomer.

Design Flexibility:
Rated comparable to the elastomer.

Installation:
Compact package judged excellent for installation.

Weight:
Rating reduced due to axial structural member.

Risk:
Somewhat better than the unconstrained elastomer but still considered relatively risky.

Summary:
Constrained elastomers should alleviate problems associated with axial/lateral straining, but as with the unconstrained elastomer, development testing is required.
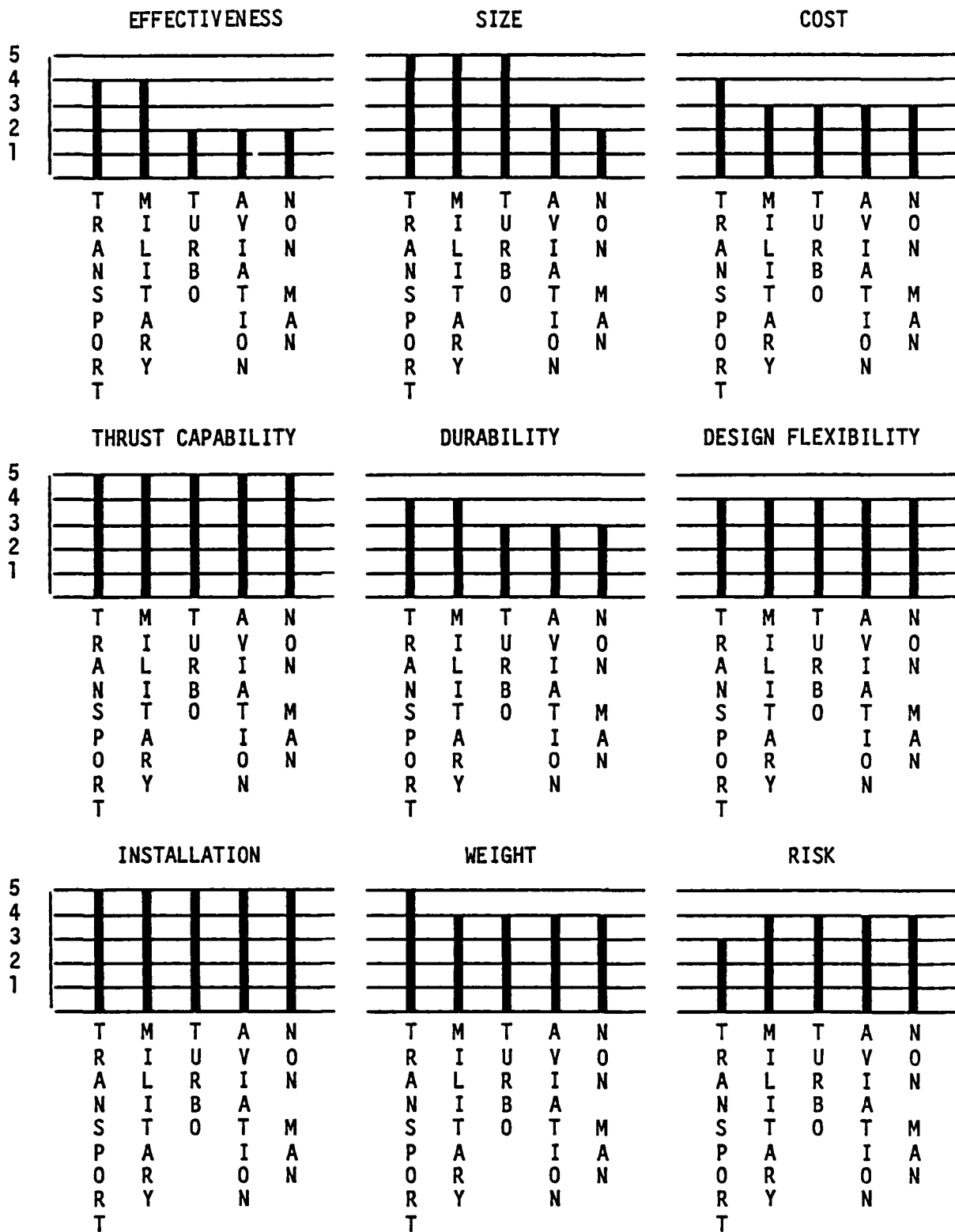
Figure 10   Constrained Elastomer Damper Ranking

4.2.4 Hybrid Boost Bearing (Figure 11)

Effectiveness: Lateral damper is conventional squeeze film design which has demonstrated effectiveness.

Size: Axial fluid film thrust bearing places restrictions on axial room available.

Cost: Relative cost is high based on dual-action system requiring separate oil feeds.

Thrust Capability: Downrated due to lack of bi-directional capability plus unknowns associated with noncontact sealing of the thrust bearing.

Durability: Rated very good overall.

Design Flexibility: Relative flexibility judged moderate based on added complexity.

Installation: Rated difficult relative to other concepts.

Weight: More relative weight due to addition of thrust bearing and resulting separate oil regulator.

Risk: Moderate.

Summary: Design suffers from need for separate oil feed system. In addition, high flow requirements needed to react high thrust load could be prohibitive.
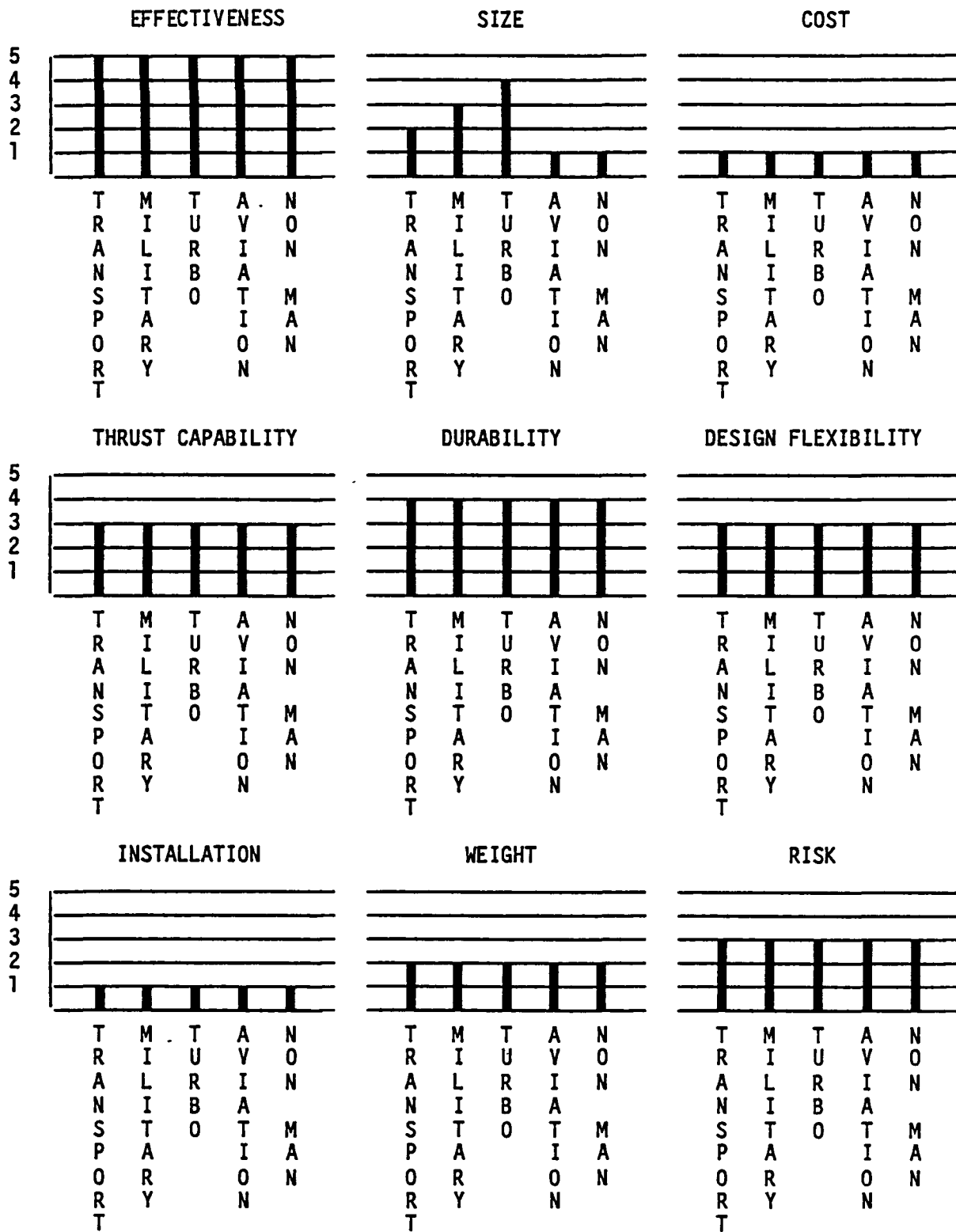
Figure 11   Hybrid Boost Bearing Ranking

4.2.5 Hydraulic Thrust Piston (Figure 12)

Effectiveness: Conventional squeeze film damper design results in very good effectiveness.

Size: As in the hybrid boost, use of the axial piston affects available axial room.

Cost: Comparable to the hybrid boost.

Thrust Capability: Good for unidirectional loading only. Seals provide better ability to control axial load.

Durability: Very good since it is based on proven squeeze film design.

Design Flexibility: Considered moderate relative to other concepts.

Installation: Rated low due to sealing requirements, number of components, and oil supply.

Weight: Slightly heavier than the hybrid boost. Very heavy relative to concepts in general.

Risk: Use of conventional squeeze film, piston ring arrangement implies low risk due to established reliability and prediction capabilities.

Summary: Comparable to the hybrid boost, but somewhat more predictable.
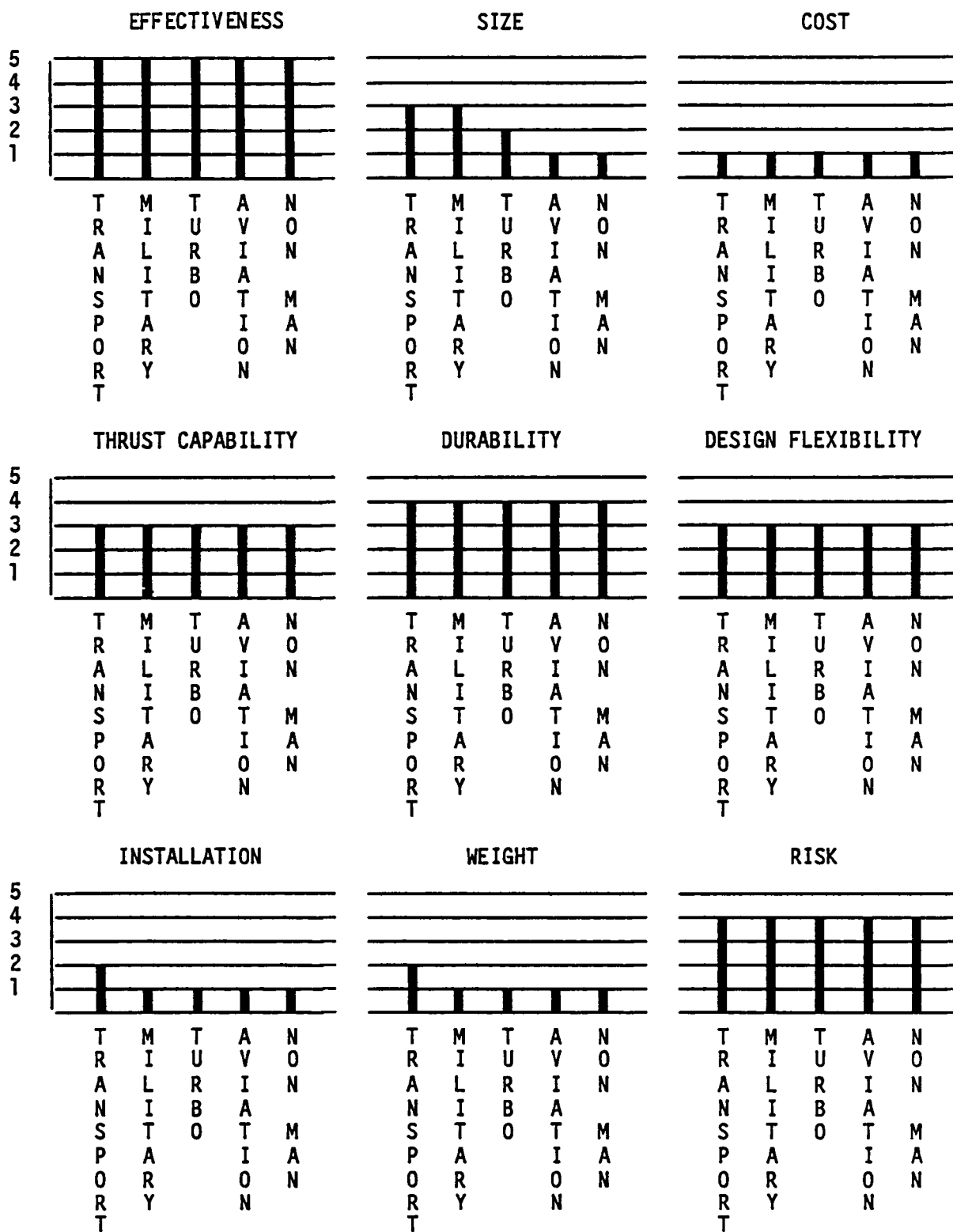
Figure 12   Hydraulic Thrust Piston Ranking

4.2.6 Conical Squeeze Film (Figure 13)

Effectiveness:	Analytically shows ability to meet lateral stiffness and damping requirements within available space.
Size:	Rated high due to radial/axial compactness. This rating is downrated for smaller engines.
Cost:	Rated very good due to simplicity.
Thrust Capability:	Concept suffers from inability to take bi-directional thrust.
Durability:	Rated very good since it employs existing technology.
Design Flexibility:	Rated high since dynamic change can be accomplished via clearance adjustments.
Installation:	Rated good to very good relative to other concepts.
Weight:	Compactness results in lightweight structure.
Risk:	Concept is a rather simple variation of demonstrated technology. Risk is assumed to be low.
Summary:	Though conceptually the concept looks good, behavior prediction is complicated by clearance changes due to speed varying thrust load.
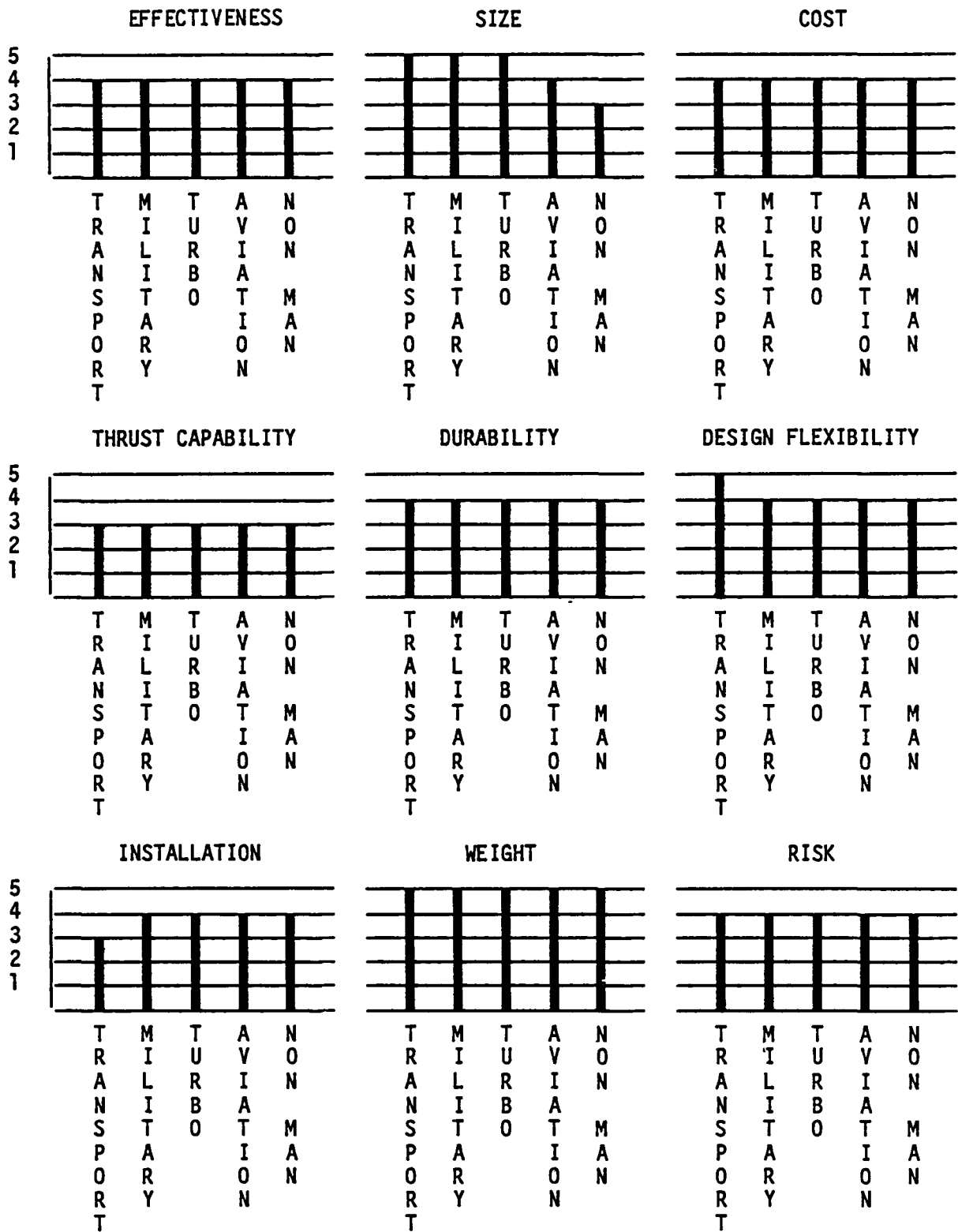
Figure 13   Conical Squeeze Film Ranking

4.2.7 Rolling Element Thrust Face (Figure 14)

LF

:iffness/damping requirements can adequately be
? of conventional squeeze film for larger damp-
rements or with a leaf spring for lower damping
1ts.

) be excellent for engines with large compart-
. Rating is reduced for small size engines.

:lement adds to the cost of the concept.

) be very good.

)w for high thrust engines due to concerns for
element durability.

:o be excellent.

?d due to multi-piece assembly.

ely low weight.

:ed somewhat due to inherent fears associated with
:ing friction surfaces.

tive concept for low thrust engines. The 'aspirin'
rolling elements are favored over the ball bear-
e to better distribution of contact load.
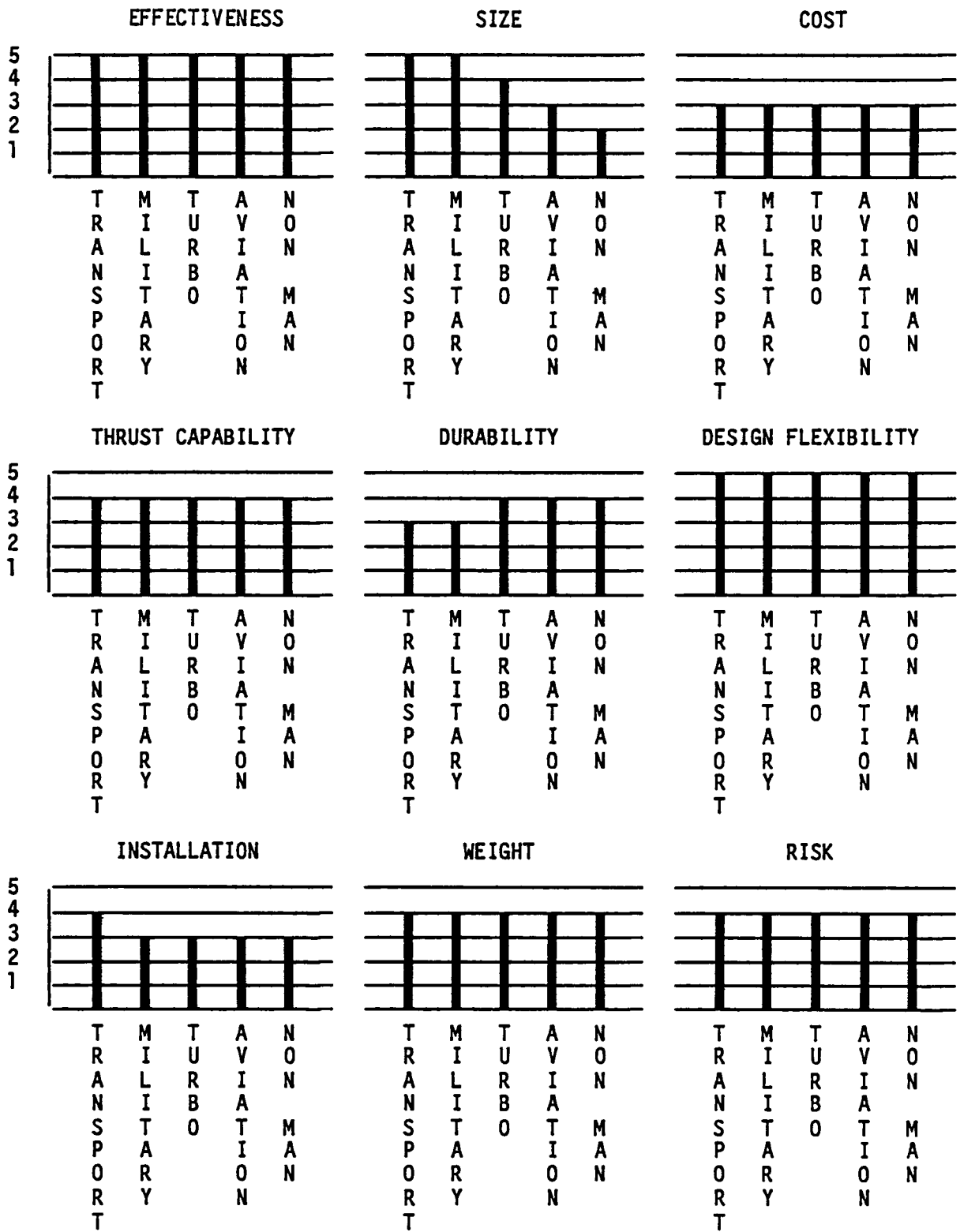
Figure 14   Rolling Element Thrust Face Ranking

4.3 Damper Selection

4.3.1 Weighting Factors

Ranking gives a general evaluation of how well each assessment parameter is satisfied without regard to relative importance of each parameter. Thus, based on each particular engine classification requirements, the assessment parameters were weighted relative to each other. The resulting evaluation is shown in Table II.

Table II

Weighting Factors

	Effec- tiveness	Size	Cost	Thrust Capa- bility	Dura- bility	Design Flex	Install	Weight	Risk
Large Transport	0.12	0.01	0.15	0.09	0.15	0.09	0.09	0.15	0.15
Military	0.12	0.09	0.10	0.09	0.09	0.09	0.12	0.15	0.15
Turboshaft	0.11	0.11	0.11	0.10	0.13	0.10	0.10	0.11	0.13
Small Gen. Aviation	0.08	0.12	0.15	0.12	0.08	0.12	0.12	0.09	0.12
Non-Manrated	0.10	0.16	0.16	0.10	0.02	0.10	0.10	0.16	0.10

4.3.2 Concept Selection

Based on the rating of concepts for each engine type and establishment of weighting factors, damper selection was determined for each engine type (Table III). Results of the evaluation show the following concept selections:

Engine Type	Selected Concept
Large Transport	Curved Beam
Military	Curved Beam
Turboshaft	Conical Squeeze Film
Small General Aviation	Elastomer
Non-Manrated	Elastomer

Selection of the curved beam for the large transport and military engine is an indication of the functional and size similarities between these two groups. The same holds true for the general aviation and non-manrated engine types where the unconstrained elastomer is shown to be best. Thus, it was decided that only three analytical studies would be undertaken: examination of curved beam behavior for a large transport engine, conical squeeze film behavior for a turboshaft, and an elastomer for a small general aviation engine. This minimized the duplication of efforts and resulted in better concentration on the performance of the three selected concepts.

Table III

Concept Rating for Each Engine Type

RANKING IS ON BASIS OF 1 TO 5 IN ORDER OF INCREASING GOODNESS.

* SELECTED CONCEPT

LARGE TRANSPORT

	RANKING									RATING									
	EFFECT	SIZE	COST	THRUST	DURA	FLEX	INSTAL	WT	RISK	EFFECT	SIZE	COST	THRUST	DURA	FLEX	INSTAL	WT	RISK	TOTAL
CURVED BM	5	5	3	5	5	5	4	4	5	0.60	0.05	0.45	0.45	0.75	0.45	0.36	0.60	0.75	4.46*
ELASTOMER	4	5	5	4	4	4	5	5	2	0.48	0.05	0.75	0.36	0.60	0.36	0.45	0.75	0.30	4.10
CONST ELA	4	5	4	5	4	4	5	5	3	0.48	0.05	0.60	0.45	0.60	0.36	0.45	0.75	0.45	4.19
HYB BOOST	5	2	1	3	4	3	1	2	3	0.60	0.02	0.15	0.27	0.60	0.27	0.09	0.30	0.45	2.75
HYDRO THT	5	3	2	3	4	3	2	2	4	0.60	0.03	0.30	0.27	0.60	0.27	0.18	0.30	0.60	3.15
CONICAL S	4	5	4	3	4	5	3	5	4	0.48	0.05	0.60	0.27	0.60	0.45	0.27	0.75	0.60	4.07
ROLL ELEM	5	5	3	4	3	5	4	4	4	0.60	0.05	0.45	0.36	0.45	0.45	0.36	0.60	0.60	3.92

MILITARY

	RANKING									RATING									
	EFFECT	SIZE	COST	THRUST	DURA	FLEX	INSTAL	WT	RISK	EFFECT	SIZE	COST	THRUST	DURA	FLEX	INSTAL	WT	RISK	TOTAL
CURVED BM	5	5	3	5	5	5	4	4	5	0.60	0.45	0.30	0.45	0.45	0.45	0.48	0.60	0.75	4.53*
ELASTOMER	4	5	5	4	4	4	5	5	2	0.48	0.45	0.50	0.36	0.36	0.36	0.60	0.75	0.30	4.16
CONST ELA	4	5	3	5	4	4	5	4	4	0.48	0.45	0.30	0.45	0.36	0.36	0.60	0.60	0.60	4.20
HYB BOOST	5	3	1	3	4	3	1	2	3	0.60	0.27	0.10	0.27	0.36	0.27	0.12	0.30	0.45	2.74
HYDRO THT	5	3	1	3	4	3	1	1	4	0.60	0.27	0.10	0.27	0.36	0.27	0.12	0.15	0.60	2.74
CONICAL S	4	5	4	3	4	4	4	5	4	0.48	0.45	0.40	0.27	0.36	0.36	0.48	0.75	0.60	4.15
ROLL ELEM	5	5	3	4	3	5	3	4	4	0.60	0.45	0.30	0.36	0.27	0.45	0.36	0.60	0.60	3.99

TURBO SHAFT

	RANKING									RATING									
	EFFECT	SIZE	COST	THRUST	DURA	FLEX	INSTAL	WT	RISK	EFFECT	SIZE	COST	THRUST	DURA	FLEX	INSTAL	WT	RISK	TOTAL
CURVED BM	3	4	3	5	5	5	3	3	5	0.33	0.44	0.33	0.50	0.65	0.50	0.30	0.33	0.65	4.03
ELASTOMER	2	5	5	4	3	4	5	5	3	0.22	0.55	0.55	0.40	0.39	0.40	0.50	0.55	0.39	3.95
CONST ELA	2	5	3	5	3	4	5	4	4	0.22	0.55	0.33	0.50	0.39	0.40	0.50	0.44	0.52	3.85
HYB BOOST	5	4	1	3	4	3	1	2	3	0.55	0.44	0.11	0.30	0.52	0.30	0.10	0.22	0.39	2.93
HYDRO THT	5	2	1	3	4	3	1	1	4	0.55	0.22	0.11	0.30	0.52	0.30	0.10	0.11	0.52	2.73
CONICAL S	4	5	4	3	4	4	4	5	4	0.44	0.55	0.44	0.30	0.52	0.40	0.40	0.55	0.52	4.12*
ROLL ELEM	5	4	3	4	4	5	3	4	4	0.55	0.44	0.33	0.40	0.52	0.50	0.30	0.44	0.52	4.00

Table III (continued)

Concept Rating for Each Engine Type

* SELECTED CONCEPT

SMALL GENERAL AVIATION

	RANKING									RATING									
	EFFECT	SIZE	COST	THRUST	DURA	FLEX	INSTAL	WT	RISK	EFFECT	SIZE	COST	THRUST	DURA	FLEX	INSTAL	WT	RISK	TOTAL
CURVED BM	3	3	3	5	5	5	3	3	5	0.24	0.36	0.45	0.60	0.40	0.60	0.36	0.27	0.60	3.88
ELASTOMER	2	4	5	4	3	4	5	5	3	0.16	0.48	0.75	0.48	0.24	0.48	0.60	0.45	0.36	4.00*
CONST ELA	2	3	3	5	3	4	5	4	4	0.16	0.36	0.45	0.60	0.24	0.48	0.60	0.36	0.48	3.73
HYB BOOST	5	1	1	3	4	3	1	2	3	0.40	0.12	0.15	0.36	0.32	0.36	0.12	0.18	0.36	2.37
HYDRO THT	5	1	1	3	4	3	1	1	4	0.40	0.12	0.15	0.36	0.32	0.36	0.12	0.09	0.48	2.40
CONICAL S	4	4	4	3	4	4	4	5	4	0.32	0.48	0.60	0.36	0.32	0.48	0.48	0.45	0.48	3.97
POLL ELFM	5	3	3	4	4	5	3	4	4	0.40	0.36	0.45	0.48	0.32	0.60	0.36	0.36	0.48	3.81

NON-MANRATED

	RANKING									RATING									
	EFFECT	SIZE	COST	THRUST	DURA	FLEX	INSTAL	WT	RISK	EFFECT	SIZE	COST	THRUST	DURA	FLEX	INSTAL	WT	RISK	TOTAL
CURVED BM	2	2	3	5	5	5	3	3	5	0.20	0.32	0.48	0.50	0.10	0.50	0.30	0.48	0.50	3.38
ELASTOMER	2	3	5	4	3	4	5	5	3	0.20	0.48	0.80	0.40	0.06	0.40	0.50	0.80	0.30	3.94*
CONST ELA	2	2	3	5	3	4	5	4	4	0.20	0.32	0.48	0.50	0.06	0.40	0.50	0.64	0.40	3.50
HYB BOOST	5	1	1	3	4	3	1	2	3	0.50	0.16	0.16	0.30	0.08	0.30	0.10	0.32	0.30	2.22
HYDRO THT	5	1	1	3	4	3	1	1	4	0.50	0.16	0.16	0.30	0.08	0.30	0.10	0.16	0.40	2.16
CONICAL S	4	3	4	3	4	4	4	5	4	0.40	0.48	0.64	0.30	0.08	0.40	0.40	0.80	0.40	3.90
POLL FLEM	5	2	3	4	4	5	3	4	4	0.50	0.32	0.48	0.40	0.08	0.50	0.30	0.64	0.40	3.62

SECTION 5.0

ANALYTICAL METHODS AND EVALUATION

5.1 Damper Equations

5.1.1 Curved Beam Damper

The curved beam damper concept, whether designed to take axial thrust or not, maintains the same lateral stiffness and damping equations. A key feature of the curved beam damper is its ability to remain fairly linear over the entire operating range of deflection and speed (Reference 2). The curved beam damper, which is patented by Pratt & Whitney (Reference 16), derives its radial stiffness from the curved beams while viscous damping is obtained from the pressure drop through the inlet and outlet ports (Figure 15).
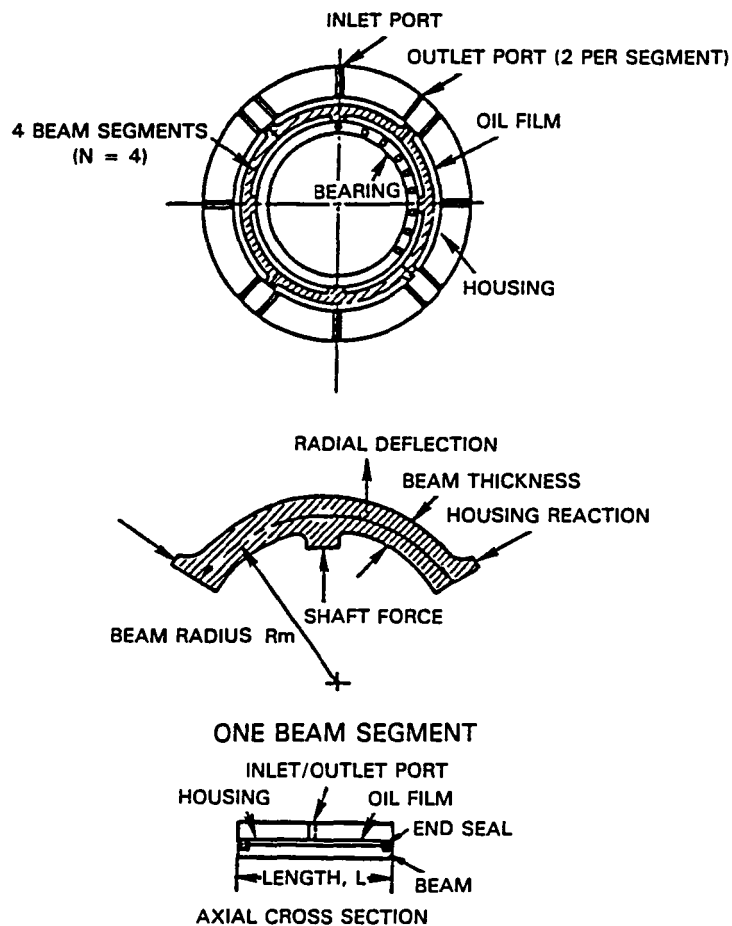
Figure 15   Curved Beam Damper

5.1.1.1 Axial Stiffness

Axial motion is reacted by rails (Figure 16) which transmit load from the outer bearing ring lugs through the rail and to a reaction lug attached to the damper support. Axial stiffness of the concept is inherently high. The main design concern is shear capability of the lugs which can be written in terms of the required shear area as follows:

area per lug = thrust load/(shear strength x N)

where N = the number of curved beams.

• Thrust Loads Are Carried by Lateral Posts
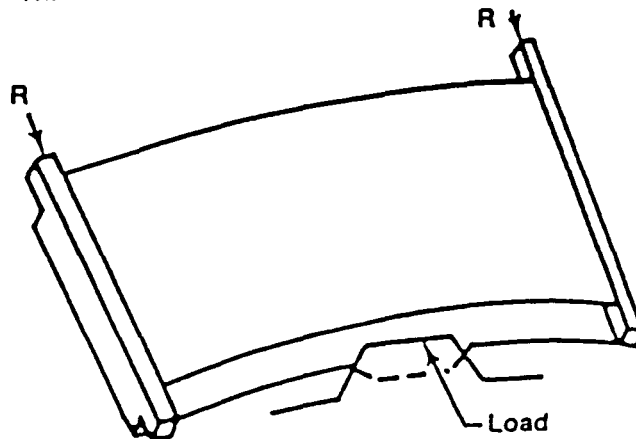
Figure 16   Thrust Loads are Carried by Lateral Posts

5.1.1.2 Lateral Stiffness

The radial stiffness calculation is a two step process. In the first step, the force deflection characteristics of the beam are determined. In the second step, the total radial force acting on the shaft is calculated by taking into account the angular position of each beam with respect to the center of the shaft.

Force deflection characteristics are based on small deflection theory, which is linear over the deflection range. Beam geometry (length, curvature, thickness and width), end conditions (guided, fixed, etc.) and material properties (Young's modulus) determine the force deflection characteristics, while the number of beams determines the total effective stiffness in the system.

29

Assuming that the beams are segmented (and thereby behave like a pin-pin beam), the force deflection characteristics can be given as:

$$\text{FORCE} \; \alpha \; \frac{Et^3 L_i}{Rm^3} \; \times \; \text{deflection}$$

$$\text{or Stiffness is proportional to} \; \frac{Et^3 L}{Rm^3}$$

where E = Young's modulus,
t = beam thickness,
L_i = segment length, and
Rm = mean beam radius.

If the number of segmented beams is N, then the effective total stiffness $(k) = A_1 \; Et^3/Rm^3$; where A_1, the constant of proportionality, depends on the number of beams (N).

5.1.1.3 Viscous Damping

In this concept, fluid is pumped through the supply and exhaust ports when shaft motion is transmitted to the curved beam. The total hydrodynamic pressure in the film is generated by two mechanisms: shearing the fluid within the clearance and pumping the fluid through the ports. The pressure generated by shearing the fluid can be modeled by the Reynolds equation and it is nonlinear. The pressure from pumping the fluid through the ports can be made proportional to the velocity of the fluid and it is linear. However, the nonlinear effect is minimized by using a relatively large clearance. Since the overall trend is to pump fluid back into the supply line, the outlet ports are kept small in order to maintain a uniform pressure distribution over the curved beam. The only purpose for the outlet port is to ensure initial filling of the fluid cavity. Similarly, the supply pressure should be greater than the pressure drop in the port, otherwise the cavity will not be refilled and starvation will occur.

The following steps are used to calculate the damping coefficient of the curved beam damper:

o Knowing the velocity, eccentricity, clearance and port properties, pressure profile over the curved beam is calculated (both squeezing and pumping).

o The forces acting on the beam are determined by integrating the profile over the area.

o All of the beam forces which are tangential to the shaft center are vectorially added.

o The damping coefficient, i.e., tangential force per unit velocity, is calculated.

30

In the current study, nonlinearity is minimized by using a relatively large clearance damper and maintaining supply pressure above the port pressure drop, thereby avoiding starvation. In such instances, it can be shown that Tangential Force α Port Flow Coefficient x Shaft Center Velocity x Beam Area.

If the port flow coefficient is constant over the operating range, then the tangential force is linearly proportional to the velocity and a constant coefficient of damping is obtained.

5.1.2 Conical Squeeze Film Equations

5.1.2.1 Axial Load Capability

Axial load reaction is supplied by the projected axial area of the damper and the current oil supply pressure defined as follows:

Damper Axial Force = Supply Pressure x Axial Area of Damper Surface.

It is assumed that multiple, large oil supply holes exist, thus alleviating pressure loss through the orifices.

5.1.2.2 Dynamic Stiffness and Damping

The main intent of the conical squeeze film concept was to allow transfer of axial load without the use of a centering spring. Thus, analytical complications arise due to possible noncentered whirl of the rotor. For the intent of this study it was assumed that, under normal operation, orbits are circular. This allows for straightforward modification of the standard lubrication theory equations for squeeze film dampers to account for an axially inclined damper surface. With reference to Figures 17 and 18, and assuming small angles, the clearance perpendicular to the damper faces can be defined as follows:

$$h = \bar{h} \cos(\alpha).$$

The circumferential variance of the radial clearance is:

$$\bar{h} = C - e \cos(\theta).$$

Thus, h can be redefined as:

$$h = C(1.-(e/C)\cos(\theta))\cos(\alpha).$$

For a squeeze film, the governing equation, assuming negligible axial flow is (Reference 13):

$$\frac{\partial}{\partial \theta}\left(\frac{h^3}{\mu}\frac{\partial P}{\partial \theta}\right) = -12R^2 \omega\frac{\partial h}{\partial \theta}$$

Using the definition of h and defining the eccentricity ratio as e/C results in the following equation defining the local pressure:

$$P = 12 \mu\omega \left(\frac{R}{C \cos\alpha}\right)^2 \frac{\varepsilon \sin\theta}{(\varepsilon^2+2)}\left[\frac{2 - \varepsilon \cos\theta}{(1-\varepsilon \cos\theta)^2}\right]$$
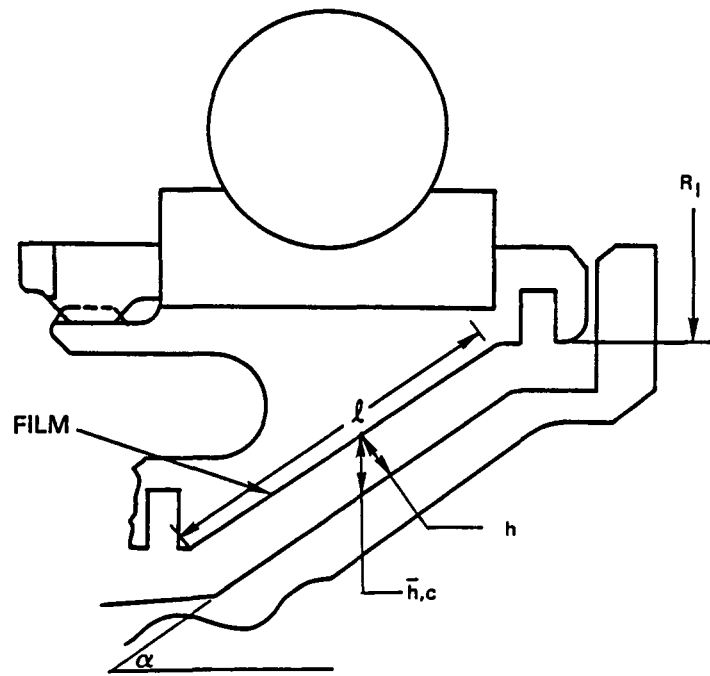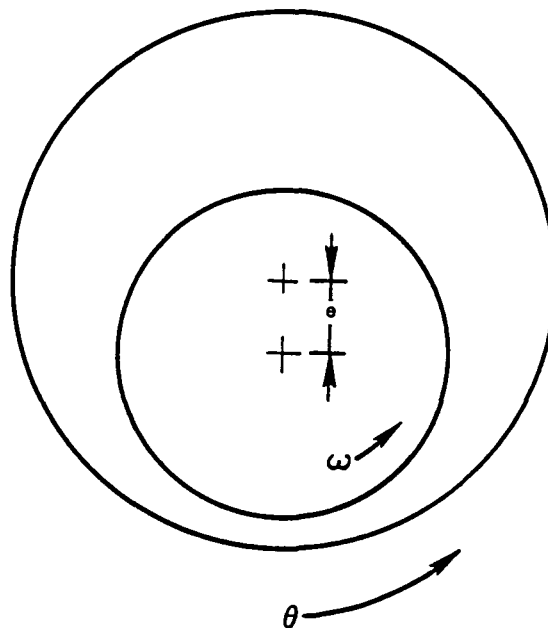
31

Figure 17   Conical Squeeze Film Damper

Figure 18   Conical Squeeze Film Analytical Solution Assumes Circular Whirl

The radius can be expressed as a function of axial position,

$$R = R_I + Z\tan(\alpha).$$

Substituting this radius equation into the pressure equation and integrating over the length and circumference results in the total radial and tangential forces for a cavitated and noncavitated damper.

	Cavitated (π Film)	Noncavitated (2π Film)
F_R	$\dfrac{(R_0{}^2+R_I{}^2)(R_0+R_I)}{4\cos^2\alpha}\dfrac{\mu l \omega}{c^2}\dfrac{24\varepsilon^2}{(2+\varepsilon^2)(1-\varepsilon^2)}$	0.0
F_T	$\dfrac{(R_0{}^2+R_I{}^2)(R_0+R_I)}{4\cos^2\alpha}\dfrac{\mu l \omega}{c^2}\dfrac{12\pi\varepsilon}{(2+\varepsilon^2)(1-\varepsilon^2)^{1/2}}$	$\dfrac{(R_0{}^2+R_I{}^2)(R_0+R_I)}{4\cos^2\alpha}\dfrac{\mu l \omega}{c^2}\dfrac{24\pi\varepsilon}{(2+\varepsilon^2)(1-\varepsilon^2)^{1/2}}$

5.1.3 Elastomer Damper Equations

Due to the extreme dependency of elastomer dynamic characteristics on the operational conditions of the engine, elastomer design is a difficult undertaking. In order to maximize the potential for arriving at a viable design, it was decided to use local cylindrical buttons, equally spaced circumferentially. This allows direct use of experimental data as well as allowing quick interchangability of button hardware during test.

Representative stiffness and damping was determined from equations and data from Reference 12. Stiffness and damping due to compression and shear, for the element shown in Figure 19, are defined as follows:

lateral stiffness $\qquad$ $K1 = Kc + Ks$

$\qquad$ where compressive stiffness $\qquad$ $Kc = \dfrac{3G'\pi D^2}{4h}\left[1 + \dfrac{\beta' D^2}{16h^2}\right]$

$\qquad$ and shear stiffness $\qquad$ $Ks = \dfrac{G'\pi D^2}{4h}$

lateral damping $\qquad$ $B1 = Bc + Bs$

$\qquad$ where compressive stiffness $\qquad$ $Bc = \dfrac{3G''\pi D^2}{4h}\left[1 + \dfrac{\beta'' D^2}{16h^2}\right]$

$\qquad$ and shear stiffness $\qquad$ $Bs = \dfrac{G''\pi D^2}{4h}$

where   D = button diameter (m)
           h = button height (m)
          G' = shear storage modulus (N/m sq)
          G" = shear loss modulus (N/m sq)
    β',β'' = shape factors determined from test.
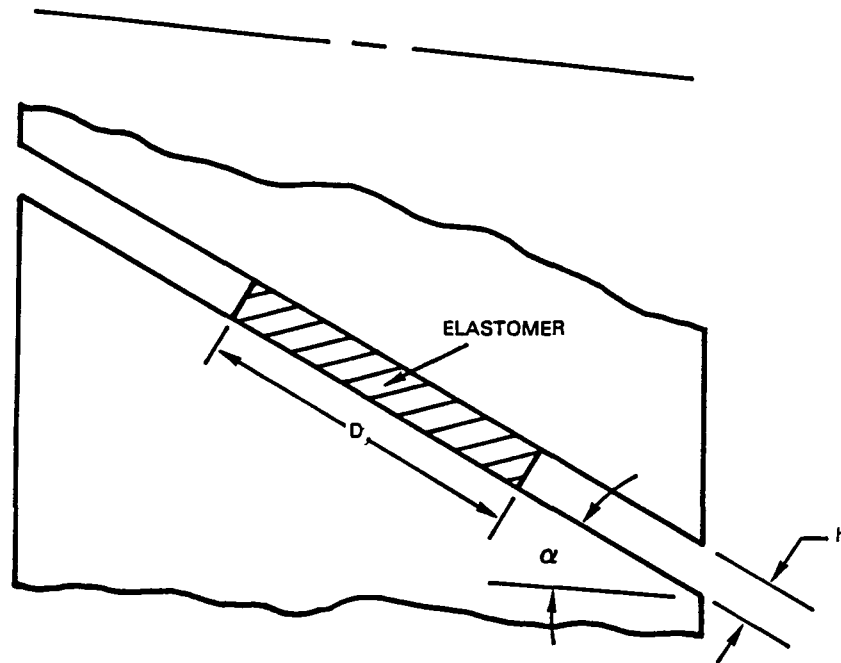
Figure 19   Elastomer Geometry

G', G", β', β'' are material related properties gained from test data. Due to damping capabilities, in-house testing, plus the ability to withstand the bearing compartment environment, Viton 70 was chosen as the material for use in the engine. Per Reference 12 data, the above material dependent coefficients can be defined as functions of frequency (ω), temperature (degrees K), and strain (ϵ).

$$G' = \frac{T}{306} \times 10^{\left[6.31 +.149 \left(\frac{2711-8.9T}{T+204} + \log_{10}\omega\right) - .115 \log_{10}\epsilon - .0159 \left(\log_{10}\epsilon\right)^2\right]}$$

$$G'' = \frac{T}{306} \times 10^{\left[5.31 + .389 \left(\frac{2711-8.9T}{T+204} + \log_{10}\omega\right) - .135 \log_{10}\epsilon - .179 \left(\log_{10}\epsilon\right)^2\right]}$$

34

$$\beta' = 10^{\left[.615 - .142 \log_{10}\omega + 2.13 \log_{10}\left(\frac{T}{306}\right) - .0837 \log_{10}\epsilon\right]}$$

$$\beta' = 10^{\left[.884 - .180 \log_{10}\omega + 1.29 \log_{10}\left(\frac{T}{306}\right) - .101 \log_{10}\epsilon\right]}$$

5.1.3.1 Total Dynamic Stiffness and Damping

Total stiffness and damping are a function of the number of buttons plus the circumferential and axial angular orientation. These are defined as follows:

total stiffness $\qquad$ $Kt = Xc\ Kc + Xs\ Ks$

total damping $\qquad$ $Bt = Xc\ Bc + Xs\ Bs$

where $\quad$ Nc = number of circumferential buttons

θ = circumferential angular location of button

α = axial inclination of button

$Xc = (Nc/2)\ \cos\alpha$

$$Xs = \sum_{i=1}^{Nc}\left[\sin\left(\frac{360\,i}{N_c}\right)\left[\sin^2\left(\frac{360\,i}{N_c}\right) + \left(\cos\left(\frac{360\,i}{N_c}\right)\sin\alpha\right)^2\right]^{1/2}\right]$$

5.1.3.2 Static Lateral Stiffness

In-house testing together with Reference 16 confirmation have shown that the shear modulus for Viton 70 is 1.38 MN/m^2 (200 psi). The compression modulus is related to the shear modulus by its Poisson's ratio (typically .5) and the elastomer shape factor,

$$Ec = 3.\ G\ (\ 1. + .07\ (D/h)\ )$$

The local button compression and shear stiffness are defined as follows:

$$Kc = A\ Ec/h$$

$$Ks = A\ G/h$$

The static lateral stiffness can be defined, as with the dynamic, as follows:

total stiffness $\qquad$ $Kt = Xc\ Kc + Xs\ Ks$

total damping $\qquad$ $Bt = Xc\ Bc + Xs\ Bs$

5.1.3.3 Axial Stiffness

The axial stiffness is a function of the combined compressive and shear stiffness:

axial stiffness $\quad$ Ka = (A Nc/h)(Ec sin(α) + G cos(α)

where A = button area (m^2).

5.2 Engine Models

In order to analytically evaluate the chosen damper concepts, engine models were developed which are representative of current designs. Each engine has a critical shaft mode in the operating range to allow evaluation of particular damping concepts.

5.2.1 Large Transport/Military Engines

Engines in this class are generally dual rotor turbofans or turbojets with thrust ratings in the 53,380 to 270,000 N (12,000 to 60,000 lb) range with operating speeds under 20,000 rpm. The model chosen for the engine study is a dual rotor turbofan for military or commercial transports. The model is the same as that analyzed under the high load damper study of Reference 3, which describes the model as follows:

Type of Engine:	Dual Spool Turbofan
Thrust:	222,000 N (50,000 lb)
Speed:	Low Rotor 1000 - 3800 rpm
	High Rotor 4700 - 8500 rpm
Dimensions:	Length 394 cm (155 in.)
	Diameter 244 cm (96 in.)
Number of Stages:	Fan 1
	Low-Pressure Compressor 4
	High-Pressure Compressor 11
	High-Pressure Turbine 2
	Low-Pressure Turbine 4
Low Rotor Weight:	1040 kg (2300 lb)
High Rotor Weight:	590 kg (1300 lb)
Engine Weight:	4080 kg (9000 lb)

The line diagram for the large transport engine model is presented in Figure 20. The low rotor for this model includes the fan, low-pressure compressor and the low-pressure turbine. It is approximately 330 cm (130 in.) long and supported on two bearings. The high rotor consists of the high-pressure compressor and the high-pressure turbine. It measures 165 cm (65 in.) and is supported on two bearings. The assumed stiffnesses for all four bearings are listed in Table IV. As shown in Figure 20, the large transport engine was modeled as a six line system for critical speed and forced response analyses.
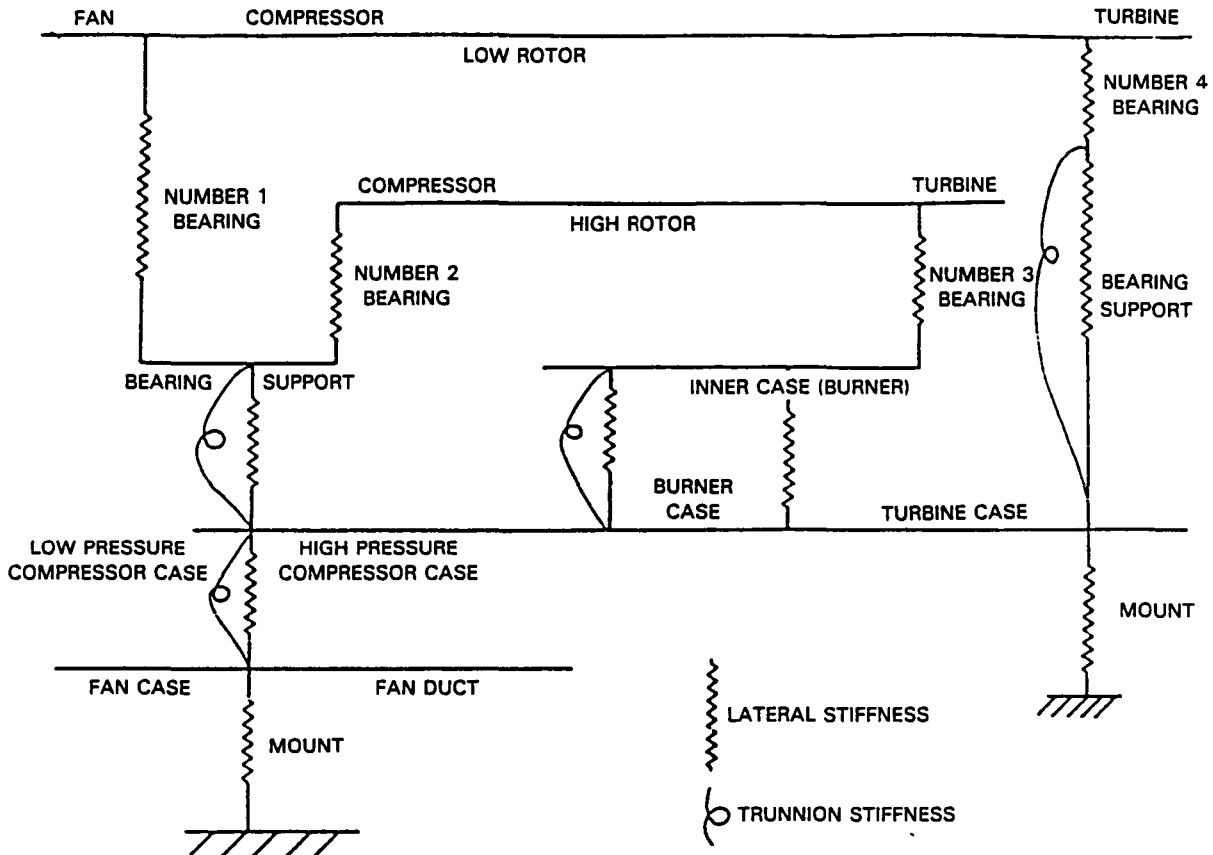
Figure 20   Line Diagram for Large Transport Engine Model

Table IV

Assumed Stiffnesses for Large Transport Engine Bearings

Bearing Number	Type	Location	Assumed Stiffness MN/m (lb/in)
1	Ball	Low Rotor	390 (2.2×10^6)
2	Ball	High Rotor	310 (1.76×10^6)
3	Roller	High Rotor	160 (9.2×10^5)
4	Roller	Low Rotor	150 (8.5×10^5)

5.2.2 Small General Aviation/Non-Manrated Engines

This class of engines includes turbojets and turbofans with a thrust rating up to 15,570 N (3,500 lb) and operating speeds to 100,000 rpm. As in the large transport engine model selection, the small general aviation model used in Reference 3 was used for this study. The model is of a single spool turbojet with the following characteristics:

Type of Engine:	Single Spool Turbojet
Thrust Rating:	13,340 N (3,000 lb)
Speed:	9,000 - 20,000 rpm
Dimensions:	Length 178 cm (70 in.)
	Diameter 56 cm (22 in.)
Number of Stages:	Compressor 9
	Turbine 2
Rotor Weight:	70 kg (150 lb)
Engine Weight:	200 kg (450 lb)

The line diagram for the small general aviation engine model is shown in Figure 21. The rotor, which includes the compressor and turbine, is approximately 127 cm (50 in.) long and supported on three bearings (Table V). This engine was modeled as a two line system for dynamic analyses.

Figure 21 Line Diagram for the Small General Aviation Engine Model

Table V

Assumed Stiffnesses for Small General Aviation Engine Bearings

Bearing Number	Type	Assumed Stiffness MN/m (lb/in)
1	Roller	64 (3.64 x 10^5)
2	Ball	43 (2.45 x 10^5)
3	Roller	28 (1.6 x 10^5)

5.2.3 Turboshaft Engines

This class comprises engines in the 370 to 11,000 kW (500 to 15,000 shp) range with operating speeds up to 50,000 rpm. The model selected is for a turboshaft engine for military and commercial applications. The engine characteristics are as follows:

Type of Engine:	Turboshaft
Thrust Rating:	9,000 kW (12,000 shp)
Speed Power Rotor:	4,500 - 10,800 rpm
Dimensions:	Length 173 cm (68 in.)
	Diameter 89 cm (35 in.)
Number of Stages:	Power shaft 3
	Drive compressor 12
	Drive turbine 2
Power Shaft Weight:	90 kg (200 lb)
Drive Shaft Weight:	122 kg (270 lb)
Total Engine Weight:	816 kg (1,800 lb)

The line diagram for the turboshaft engine model is shown in Figure 22. In this model the power shaft comprises the shaft and turbine. Front-end coupling to gear system has not been included. The shaft is 165 cm (65 in.) long and supported by two bearings. Thrust is taken by an aft end ball bearing. The drive rotor consists of a compressor and turbine. It is 127 cm (50 in.) long and supported on two bearings. The assumed bearing stiffnesses are listed in Table VI. As shown in Figure 22, the engine is modeled as a 4-line system for dynamic analysis.

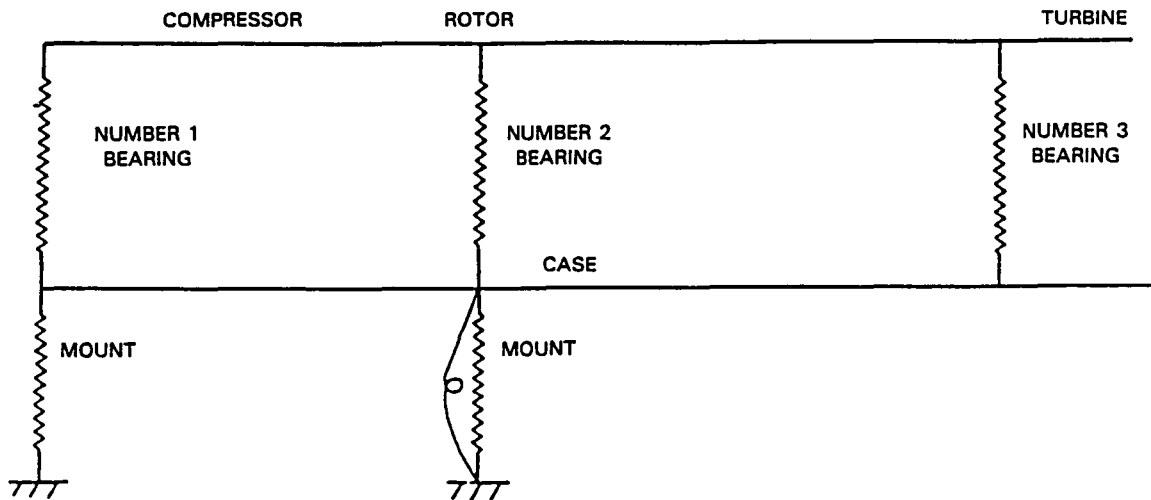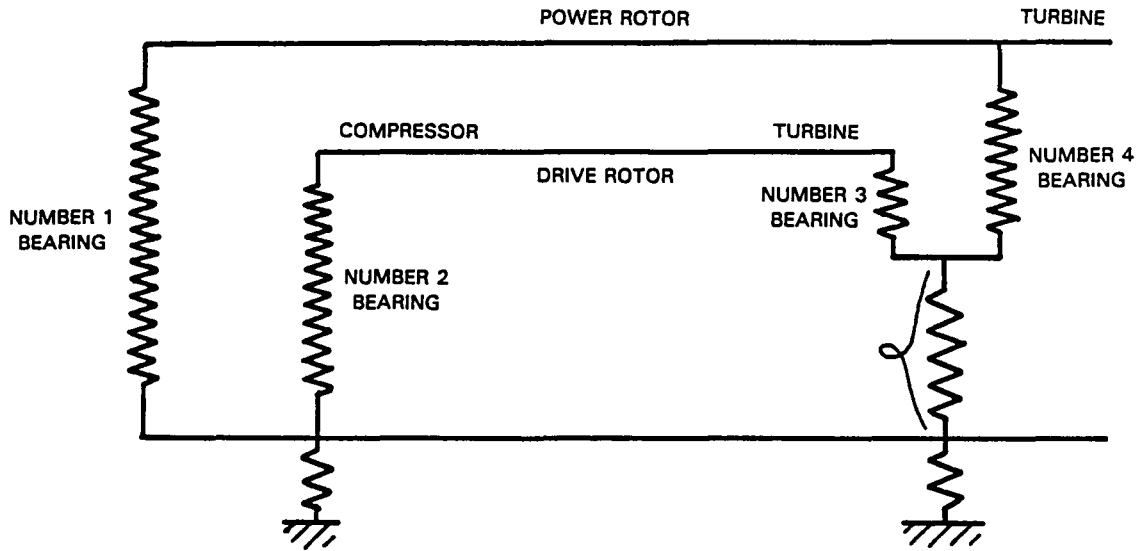Figure 22   Line Diagram for the Turboshaft Engine Model

Table VI

Assumed Stiffnesses for Turboshaft Bearings

Bearing Number	Type	Location	Assumed Stiffness MN/m (lb/in)
1	Roller	Power	114 (0.65 x 10^6)
2	Ball	Drive	131 (0.75 x 10^6)
3	Roller	Drive	88 (0.50 x 10^6)
4	Ball	Power	245 (1.40 x 10^6)

5.3 Critical Speed Analysis

In order to define critical speed placement throughout the operating range, full system flexural natural frequencies are calculated. A brief description on the use of critical speeds during the design phase is in Reference 3. The intent in this study was to isolate the key rotor modes which have significant strain energy at a thrust bearing which suggests a mode sensitive to imbalance and thus a good location for external damping.

The critical speed analysis used in this study is based on the Prohl approach (Reference 14). The steady state variables (deflection, slope, moment and shear) at lumped mass stations are defined by the transfer matrix method. Rotors, stators, and intermediate support structures are modeled as lines. Each line consists of a number of mass stations connected by massless spring elements. The mass stations account for inertia and gyroscopic effects, while the spring elements represent bending and shear flexibilities. A beam bending approximation is used to calculate flexibilities between mass stations. Connections between two lines are defined by solving the shear force and moment equations at the joints. A characteristic determinant is obtained and a speed search is conducted to identify the critical speeds at which the determinant goes to zero. The critical speeds are then substituted back into the transfer matrix to generate the deflections, slopes, moments and shear forces at all the mass stations. The mode shape is defined by deflection and slope. Once this definition is complete, the percent distribution by kinetic energy and strain energy in each of the components is calculated.
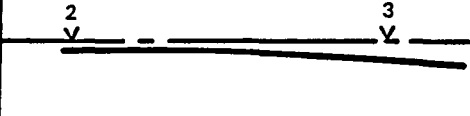
Results of the analysis for each of the representative engines are presented in the following sections.

5.3.1 Transport Engine

Fifteen critical speed modes were calculated for the transport engine. A high compressor mode at 7783 rpm was selected for evaluation. This mode is a principal pitch mode of the rotor with significant strain energy in the high rotor and forward (thrust) bearing. This mode was evaluated in Reference 3 for high load damping capabilities. Modes are shown in Figure 23. For ease of visualization, only the rotor of concern (high rotor) is shown in the mode shape. Key energy participation is listed adjacent to the mode shape.

HIGH ROTOR CRITICAL SPEEDS

BELOW IDLE

SPEED	MODE SHAPE (HIGH ROTOR)	ENERGY DISTRIBUTION		
		HIGH ROTOR	LOW ROTOR	CASE STRUCTURE
1334		KINETIC ENERGY = 18% STRAIN ENERGY = 1% BEARING NO 2 = 0% BEARING NO 3 = 1%	28% 8% NO 1 0% NO 4 1%	54% 89%
1963		KINETIC ENERGY = 5% STRAIN ENERGY = 1% BEARING NO 2 = 0% BEARING NO 3 = 1%	72% 77% NO 1 1% NO 4 2%	25% 18%
2161		KINETIC ENERGY = 2% STRAIN ENERGY = 1% BEARING NO 2 = 0% BEARING NO 3 = 0%	20% 11% NO 1 0% NO 4 1%	78% 86%
2746		KINETIC ENERGY = 35% STRAIN ENERGY = 2% BEARING NO 2 = 0% BEARING NO 3 = 8%	4% 2% NO 1 0% NO 4 1%	61% 87%
3512		KINETIC ENERGY = 7% STRAIN ENERGY = 1% BEARING NO 2 = 1% BEARING NO 3 = 2%	44% 22% NO 1 0% NO 4 2%	49% 72%
3755		KINETIC ENERGY = 16% STRAIN ENERGY = 2% BEARING NO 2 = 0% BEARING NO 3 = 7%	33% 12% NO 1 1% NO 4 5%	51% 73%

Figure 23 High Rotor Critical Speed Mode Shapes and Energy Distribution; Large Transport Engine

42

ABOVE IDLE				
SPEED	**MODE SHAPE (HIGH ROTOR)**	**ENERGY DISTRIBUTION**		
		HIGH ROTOR	**LOW ROTOR**	**CASE STRUCTURE**
4889	*(mode shape diagram, nodes 2, 3)*	KINETIC ENERGY = 3% STRAIN ENERGY = 1% BEARING NO 2 = 0% BEARING NO. 3 = 2%	71% 66% NO 1 0% NO 4 3%	26% 28%
6356	*(mode shape diagram, nodes 2, 3)*	KINETIC ENERGY = 5% STRAIN ENERGY = 1% BEARING NO. 2 = 0% BEARING NO 3 = 6%	18% 11% NO 1 0% NO 4 3%	77% 79%
7713	*(mode shape diagram, nodes 2, 3)*	KINETIC ENERGY = 8% STRAIN ENERGY = 4% BEARING NO 2 = 2% BEARING NO. 3 = 0%	68% 39% NO 1 0% NO 4 25%	24% 30%
7783	*(mode shape diagram, nodes 2, 3)*	KINETIC ENERGY = 72% STRAIN ENERGY = 34% BEARING NO 2 = 19% BEARING NO 3 = 0%	5% 4% NO 1 0% NO 4 3%	22% 40%	SELECTED FOR CURVED BEAM DAMPER EVALUATION

Figure 23 (Continued)

5.3.2 General Aviation Engine

Six critical speed modes were identified for the general aviation engine. A compressor mode at 14,479 was selected for the elastomer damper study due to high strain energy in the power shaft thrust bearing. Modes are shown in Figure 24.

CRITICAL SPEEDS		

BELOW IDLE		
SPEED	MODE SHAPE	ENERGY DISTRIBUTION

SPEED	MODE SHAPE	ROTOR	CASE STRUCTURE
1406	1 ˅ ʌ 2 ʌ 3	KINETIC ENERGY = 35% STRAIN ENERGY = 1% BEARING NO. 1 = 0% BEARING NO 2 = 0% BEARING NO 3 = 1%	65% 98%
2236	1 ˅ 2 ˅ 3 ˅	KINETIC ENERGY = 4% STRAIN ENERGY = 1% BEARING NO 1 = 0% BEARING NO 2 = 0% BEARING NO. 3 = 0%	96% 99%
4176	1 ˅ 2 ˅ 3 ˅	KINETIC ENERGY = 48% STRAIN ENERGY = 3% BEARING NO 1 = 2% BEARING NO 2 = 3% BEARING NO 3 = 1%	52% 91%

ABOVE IDLE		
9355	1 ˅ ʌ 2 3 ˅	KINETIC ENERGY = 68% STRAIN ENERGY = 27% BEARING NO 1 = 0% BEARING NO. 2 = 3% BEARING NO. 3 = 66%	32% 4%
14479	1 ˅ ʌ 2 ʌ 3	KINETIC ENERGY = 55% STRAIN ENERGY = 33% BEARING NO. 1 = 11% BEARING NO 2 = 43% BEARING NO 3 = 2%	45% 11%	SELECTED FOR ELASTOMER DAMPER EVALUATION
16261	1 ˅ ʌ 2 ʌ 3	KINETIC ENERGY = 43% STRAIN ENERGY = 7% BEARING NO 1 = 6% BEARING NO 2 = 8% BEARING NO 3 = 3%	57% 76%

Figure 24 Critical Speed Mode Shapes and Energy Distribution; Small General Aviation Engine

5.3.3 Turboshaft Engine

Three critical speed vibration modes were identified for the turboshaft engine. A power shaft mode at 8,909 rpm was selected for analysis of a conical squeeze film since it is a principal pitch mode of the shaft with high strain energy in both the shaft and the rear bearing. Engine power shaft modes are shown in Figure 25.
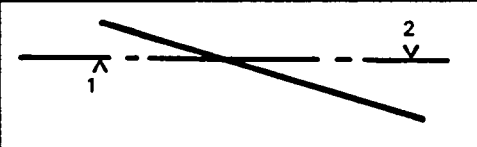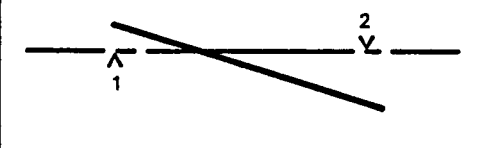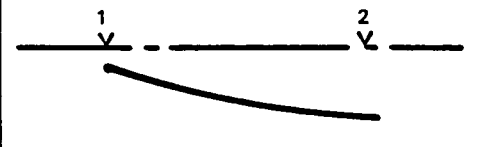
POWER ROTOR CRITICAL SPEEDS					
BELOW IDLE					
SPEED	MODE SHAPE	ENERGY DISTRIBUTION			
586	(mode shape diagram)	POWER ROTOR KINETIC ENERGY = 3% STRAIN ENERGY = 0% BEARING NO 1 = 0% BEARING NO 2 = 0%	DRIVE ROTOR 1% 0% NO 3 2% NO 4 3%	CASE STRUCTURE 96% 100%	
957	(mode shape diagram)	KINETIC ENERGY = 26% STRAIN ENERGY = 0% BEARING NO 1 = 0% BEARING NO 2 = 0%	4% 0% NO 3 0% NO 4 0%	70% 100%	
ABOVE IDLE					
8909	(mode shape diagram)	POWER ROTOR KINETIC ENERGY = 59% STRAIN ENERGY = 11% BEARING NO 1 = 1% BEARING NO 2 = 22%	DRIVE ROTOR 4% 1% No 3 1% No 4 1%	CASE STRUCTURE 37% 63%	SELECTED FOR CONICAL SQUEEZE FILM DAMPER ANALYSES

Figure 25 Power Rotor Critical Speed Mode Shapes and Energy Distribution; Turboshaft Engine

5.4 Damper Design Criteria

Engine size, purpose, and damper location place different constraints on damper requirements. This is evident since different concepts were chosen for different engine classes. A list of the particular engine damper design limitations is shown in Table VII.

Table VII

Damper Concept Limitations

	Large Transport	Small General Aviation	Turboshaft
Damper load due to gravity	1155 N (260 lb)	245 N (55 lb)	845 N (190 lb)
Axial thrust load: At critical	34,700 N (7,800 lb)	2225 N 500 lb)	9340 N (2100 lb)
At max speed	66,700 N (15,000 lb)	6670 N (1500 lb)	17,790 N (4000 lb)
Normal imbalance	144 gm-cm (2 oz-in.)	72 gm-cm (1 oz-in.)	144 gm-cm (2 oz-in.)
Blade tip-gap reduction	.08 mm (3 mils)	.08 mm (3 mils)	.13 mm (5 mils)
Case Vibration	.05 mm (2 mils)	.05 mm (2 mils)	.05 mm (2 mils)
Compartment limitations:			
Length	10.2 cm (4.0 in.)	5.1 cm (2.0 in.)	5.1 cm (2.0 in.)
Inner Diameter	30.5 cm (12.0 in.)	13.2 cm (5.2 in.)	17.8 cm (7.0 in.)
Outer Diameter	40.6 cm (16.0 in.)	17.8 cm (7.0 in.)	22.9 cm (9.0 in.)
Temperature	394°K (250°F)	394°K (250°F)	450°K (350°F)

5.4.1 Curved Beam Damper - Large Transport Engine

Compactness and weight are key requirements for large transport engine damper design, therefore, the curved beam damper was chosen for this application. The damper is located at the front of the high rotor where air inlet temperatures are below 422°K (300°F). The damper compartment is protected with minimum heat shielding.

5.4.2 Elastomer Damper - General Aviation Engine

The elastomer is located at the intermediate support location at the rear of the compressor. Temperatures exceeding 700°K (800°F) are common and adequate heat shielding is necessary to protect the elastomer as well as the bearing. Low static radial and thrust loads allow the elastomer to be an attractive concept.

5.4.3 Conical Squeeze Film - Turboshaft Engine

The conical squeeze film is required to operate at a support location aft of the power turbine section. A high temperature environment requires adequate heatshielding of the damper/bearing area. Since the conical squeeze film, as configured, is good for unidirectional axial thrust loads, the turboshaft aft support offers an advantageous location for evaluation.

5.5 Analytical Evaluation

Pratt & Whitney has developed a sophisticated steady-state forced response analysis to predict engine response under various dynamic loads (Reference 15). It is based on the standard transfer matrix method but can efficiently account for nonlinear springs, nonlinear viscous dampers, coulomb dampers, etc. As part of this study, the analysis was enhanced to include the elastomer and conical squeeze film nonlinear elements. This multishaft analysis is a widely used design tool at different stages of engine development. For a given set of forces, this analysis generates deflections, slopes, moments and shear forces at different locations over the entire speed range. The relative motion between the rotor and the case, dynamic loads through the support structure, and absolute deflections of critical case structure locations are evaluated to assure efficient and safe operation of the engine.

In this program, forced response analysis has been used to determine damper requirements and to evaluate engine dynamic response with the damper concepts which were selected.

5.5.1 Curved Beam Damper Analysis - Large Transport Engine

5.5.1.1 Axial Load Capability

Axial load carrying capability is determined by the shear area of the lugs. The dynamic analysis results show that four curved beams are required to meet sensitivity requirements. This allows four equally spaced lugs at the mid-beam location. Based on the maximum axial load of 66,700 N (15,000 lb) and a typical minimum shear strength of 345 MN/m^2 (50 ksi) for a martensitic steel, the required individual lug shear area at the bearing outer diameter and damper support is 0.48 cm^2 (0.075 in^2). This is easily attainable and allows an appreciable safety margin to be built into the lugs.

5.5.1.2 Dynamic Analysis

An extensive dynamic analysis was performed for this damper and engine in Reference 3.

Damper design parameters which resulted in attainment of design goals are shown in Table VIII.

Table VIII

Large Transport Engine

Curved Beam

Number of Beams	4
Thickness of Beam - cm (in.)	4.0 (1.59)
Oil Cavity Thickness - mm (mil)	1.02 (40)
Supply Pressure - N/m^2 (psi)	1.1×10^6 (155)
Port Pressure Drop - N/m^2 (psi)	1.2×10^6 (170)
Film Pressure - N/m^2 (psi)	1.6×10^5 (23)
Port-Flow Coefficient	0.56
Maximum Bending Stress - N/m^2 (psi)	2.0×10^8 (28,200)
Radius - cm (in.)	16.5 (6.5)
Length - cm (in.)	5.1 (2.0)
K at High Load and	
K at Low Load - MN/m (lb/in.)	88 (5×10^5)
B at High Load and	
B at Low Load - MN/m (lb/in.)	52,500 (300)

5.5.1.3 Summary

Theoretically, a curved beam damper can be designed for any application; the limiting parameters are required beam size and port coefficients. The independent stiffness and damping characteristics of the curved beam damper eliminate the common difficulty encountered in designing a squeeze film damper. Use of lugs and rails to transfer axial load results in a thrust load carrying arrangement that is both rigid and strong. The major drawback is lack of experimental verification of the analysis. Factors which should be considered to influence prediction include fluid inertia, port flow coefficient fluctuation, and the dynamics of the curved beam.

5.5.2 Elastomer Analysis - Small General Aviation Engine

Design of elastomers for aircraft engines is complicated because elastomer behavior is a function of static and dynamic strain. Significant empirical data have been reported which were used to analytically evaluate elastomer performance. However, it is assumed that engine testing of different elastomer materials and geometry is necessary; thus means to handle quick change should be allowed for in the design process. Due to this and the greater surface area for heat transfer, it was decided to design the elastomer as segmented buttons per Reference 12. This would allow for buttons of various diameters and thicknesses, as well as angular inclination to be experimentally evaluated. Use of buttons also put more credibility into the analytical process since testing has been done using this type of element.

In order to analyze elastomer effectiveness, the major damping was assumed to be isolated in the elastomer. This would hopefully add conservatism to prediction since inherent hysteretic damping of the support and case structure are not accounted for. The elastomer has to meet four main stiffness requirements for normal operation. These are: 1) a static stiffness requirement to maintain rotor position at rest, 2) dynamic stiffness and damping to meet sensitivity requirements, 3) axial stiffness to limit axial travel, and 4) preload to prevent elastomer operation in tension.

5.5.2.1 Geometry Considerations

Based on Reference 12 and in-house testing, it was decided to vary the button diameter from 2 to 2.5 cm (0.8 to 1.0 inch). The 2.5 cm restriction was made due to concerns about load dieout past the 2.5 cm bearing outer diameter ring length. Thickness variations were made from 1.59 to 4.76 mm (1/16 to 3/16 inch). The number of circumferential buttons studied was from 6 to 12. Twelve was the limit due to available circumferential length.

5.5.2.2 Lateral Static Stiffness

Static stiffness is required in order to limit the deflection of the static rotor. The maximum tip gap reduction has been set as 50 percent of the dynamic requirement or 0.05 mm (2 mil). Assuming the 0.05 mm can be translated to the bearing/damper stack, and for a gravity load of 245 N (55 lb), the lateral static stiffness requirement is 5430 N/n (31,000 lb/in.). Lateral static stiffness values were calculated for a range of elastomer parameters, Figure 26. It is shown that the stiffness requirement can easily be met with six circumferentially spaced buttons.
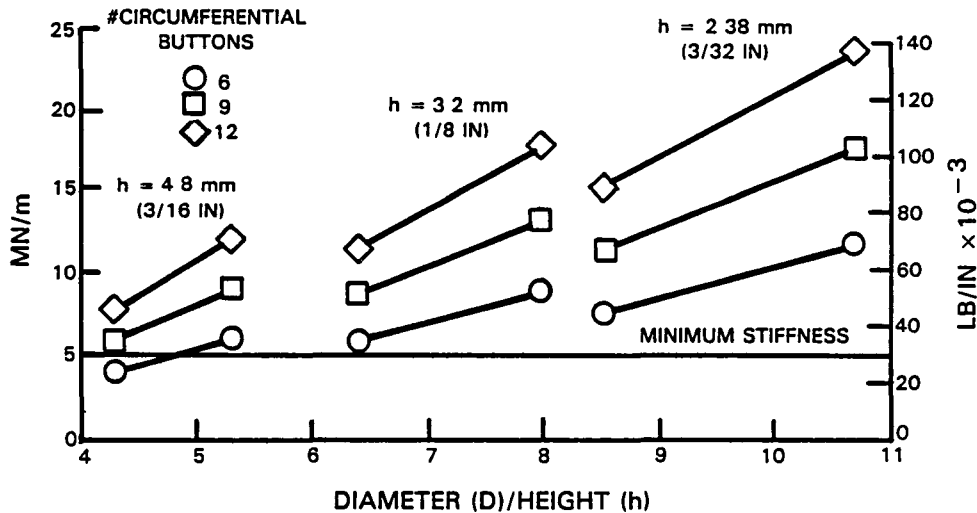

Figure 26 Lateral Static Stiffness as a Function of the Number of Circumferential Buttons, Button Diameter and Height

5.5.2.3 Preload

In order to assure that the elastomer operates in compression plus realizing that excessive preload alters the empirical data, it was decided to design to a preload value of 5 percent. This results in a 0.05 dynamic strain limit.

5.5.2.4 Axial Static Stiffness

The bearing is allowed to travel 0.7 mm (30 mil) axially. For a peak axial load of 6682 N (1500 lb), the required axial stiffness is 8756 N/m (50,000 lb/in.). An evaluation of elastomer parameters shows that 9 to 12 buttons are required as well as a thickness of 2.38 mm (0.094 in.) or less and angular inclination greater than 5 degrees (Figure 27).
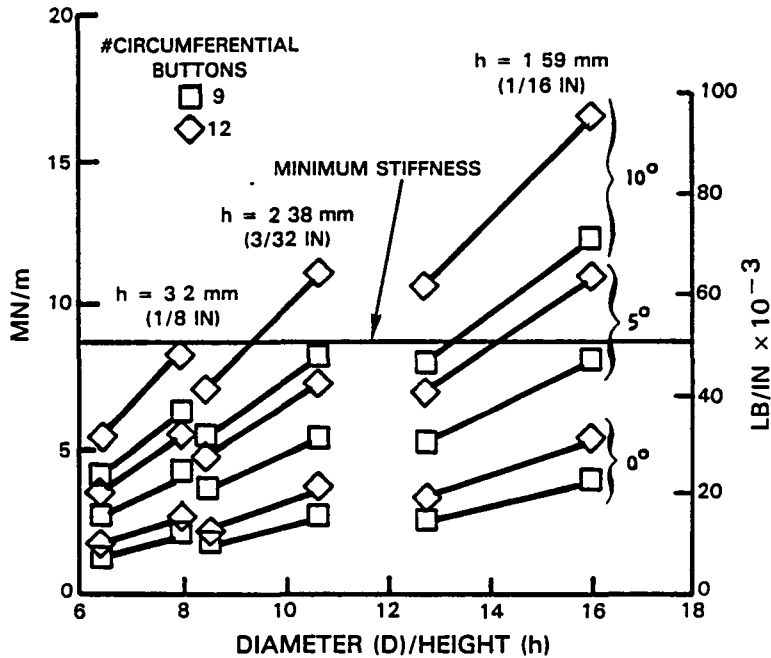
50

Figure 27   Axial Static Stiffness as a Function of Angular Inclination of Buttons, the Number of Buttons, and Button Diameter and Height

5.5.2.5 Dynamic Response

A forced response evaluation was conducted for the 14,500 rpm mode using 72 gm-cm (1 oz-in.) imbalance at the front turbine stage. Compartment temperature was assumed to be 394°K (250°F). Parametric evaluation of elastomer performance on tip gap reduction (Figure 28) and case amplitude (Figure 29) shows that a 2.38 mm (0.094 in.) thick, 2.5 cm (1 in.) diameter geometry is required for 12 buttons, or 9-12 buttons are required for an elastomer thickness of 1.587 mm (0.063 in.).
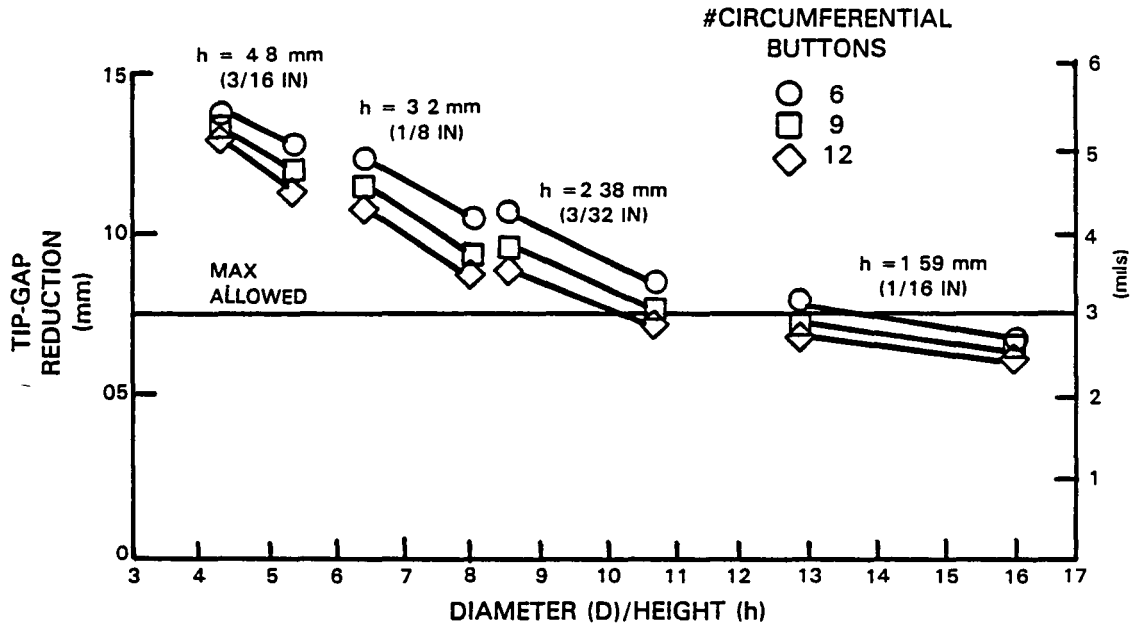
Figure 28   Effect of Elastomer Parameters on Tip Gap Reduction in Compressor
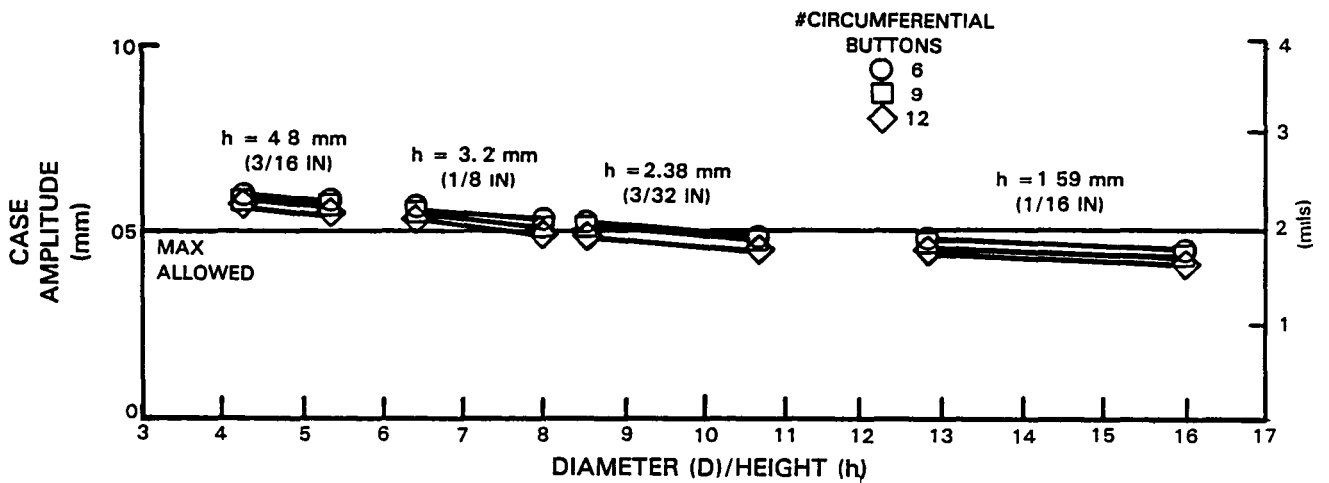Due to 72 gm-cm (1 oz-in.) Imbalance

Figure 29   Effect of Elastomer Parameters on Maximum Case Amplitude Due to 72
gm-cm (1 oz-in.) Imbalance in Compressor

5.5.2.6 Geometry Selection

Analytical evaluation results in the following design, which marginally meets our design requirements.

Table IX

Elastomer Damper Marginal Design

Number of buttons: 12
Button height: 2.38 mm (0.094 in.)
Button diameter: 2.5 cm (1.0 in.)
Angular inclination: 10 degrees

		Calculated	Requirement
Static stiffness	(MN/m)	49	5.4 min
	(lb/in.)	280,000	31,000
Axial stiffness	(MN/m)	11.1	8.8 min
	(lb/in.)	63,4000	50,000
Dynamic tip gap reduction	(mm)	.07	.076 max
	(mil)	2.87	3.0
Dynamic case deflection	(mm)	.046	.05 max
	(mil)	1.80	2.0
Dynamic elastomer strain		.004	.050

The dynamic stiffness is predicted to be 315 Mn/m (1.8x10^6 lb/in.) and damping 16,300 NS/m (93 lb-sec/in.), which represents a loss factor of 0.084 which is comparable to results of Reference 12.

The ability of the elastomer to meet life requirements can only be obtained through controlled testing which includes full environmental factors. For this particular application, in order to control sensitivity, a high stiffness was required. This resulted in low elastomer strains thus providing good potential for long service life.

5.5.2.7 High Load Evaluation

As well as meeting requirements for safe and efficient normal operation, the elastomer must also be able to limit engine response when subjected to high imbalance, principally blade loss events. An evaluation of elastomer performance was made considering loss of one blade in the compressor which represents 720 gm-cm (10 oz-in.) of unbalance. The analysis was performed using geometry for the marginal design, Table IX. Table X compares the key design requirements for maximum tip gap and bearing load and the predicted capability of the elastomer. As can be seen, the elastomer is predicted to adequately meet a blade loss condition. It is interesting to note that the dynamic strain slightly exceeds the preload strain thus demonstrating that an increased preload may be needed.

Table X

Elastomer High Load Capability

720 gm-cm (10 oz-in.) Imbalance

	Requirement	Predicted
Tip Gap Deflection	1.27 mm (50 mil)	0.79 mm (31 mil)
Bearing Load	66,700 N (15,000 lb)	28,900 N (6,500 lb)
Dynamic Strain	0.05	0.0534

5.5.2.8 Summary

Though the elastomer is predicted to meet the stated design requirements, various other factors not considered can influence the calculated dynamic properties as well as degrade the properties due to the effects of time. Among the items affecting predicted properties is the multidirectional straining of the elastomer, as well as surface straining due to thermal expansion mismatching plus adhesive effects. Testing is required to determine time related effects such as creep and fatigue. In addition, in-house testing has shown that the dynamic properties for the elastomer can significantly be reduced in time, particularly when subjected to an elevated temperature.

Additional concerns are: 1) post-run soak down increasing the compartment temperature, leading to possible short or long term deformation of the elastomer; 2) adhesive strength and durability; and 3) selection of the number of circumferential buttons such that it is not coincident with, or an integer multiple of, the rotor or stator stages in order to prohibit possible excitation of these resonances. On the plus side, the elastomer is quite attractive from a total damping view since it has the inherent ability to damp lateral displacement and slope as well as axial and torsional motion.

5.5.3 Conical Squeeze Film Analysis - Turboshaft Engine

Design of a conical squeeze film damper presents new challenges since it is susceptible to axial thrust/lateral load coupling. The design must be able to react with the use of available oil feed pressure.

5.5.3.1 Axial Thrust Load

Barring use of electronic sensors and a highly sophisticated pressure regulator system, which adds cost and risk, it is difficult to actively balance the axial thrust load with a pressure field. In order to set a design, a typical state-of-the-art oil pressure supply system is assumed. The pressure versus operating speed varies from 0.69 MN/m^2 (100 psi) at idle to 1.86 MN/m^2 (270 psi) at takeoff and is typically linear (Figure 30). The axial thrust load on the bearing is nonlinear, as shown in Figure 31. It becomes evident from these curves that for an assumed axial surface for the damper, the supply pressure will overpower the axial thrust load at low speeds, and at higher speeds the converse is true. Therefore, it is evident that thrust face washers are required in order to adequately react load. The conical squeeze film offers the ability to select an operating range which is more beneficial to alleviate axial load and thus washer wear leading to increased life. Since the mode of concern is projected to be at 8900 rpm and cruise is at 9800 rpm, it was decided to design the damper so that the pressure load and axial thrust load matched at the cruise condition. This allows potential for minimum wear during the highest cycle portion of the flight envelope by minimizing load as well as offering damping desired due to close proximity to the key critical speed. In order to meet this criteria, it was found that a 74 cm^2 (11.5 in.^{2}) axial projected area of the damper is needed resulting in a 26 degree cone angle (Figure 32). In order to minimize weight, it was decided to design to the minimum diameter of 17.8 cm (7.0 in.) as well as.to use a damper length of 2.5 cm (1.0 in.) which is typical of our experience. As can be seen in Figure 32, the pressure load will be roughly twice the axial thrust load at idle, but at takeoff the axial load will exceed the pressure load by 30 percent.

5.5.3.2 Dynamic Response

Having set key dimensions of the damper design, the next task was to determine the ability of the damper to meet the design requirements for sensitivity. The final design variable available is the damper clearance. This was varied from 0.13 to 0.5 mm (5 to 20 mils) with results shown in Figure 33. As can be seen, a damper with at least 0.33 mm (13 mil) clearance is required to meet both blade tip gap reduction and case amplitude limits of 0.13 and 0.5 mm (5 and 20 mils), respectively. A concern now becomes that of the axial travel of the inner ring due to off-balanced loading. Axial motion causes the clearance to either increase or decrease. Thus, the 0.33 mm (13 mil) clearance becomes a minimum allowable clearance to be incurred during axial contact. In order to minimize travel, it was decided to allow a total of 0.25 mm (10 mil) of axial play. This results in a centralized damper clearance of 0.38 mm (15 mil) with minimum and maximum fluctuations of 0.05 mm (2 mil). Tip gap reduction and case deflection plots for this clearance variance over the speed range are shown in Figures 34 and 35.
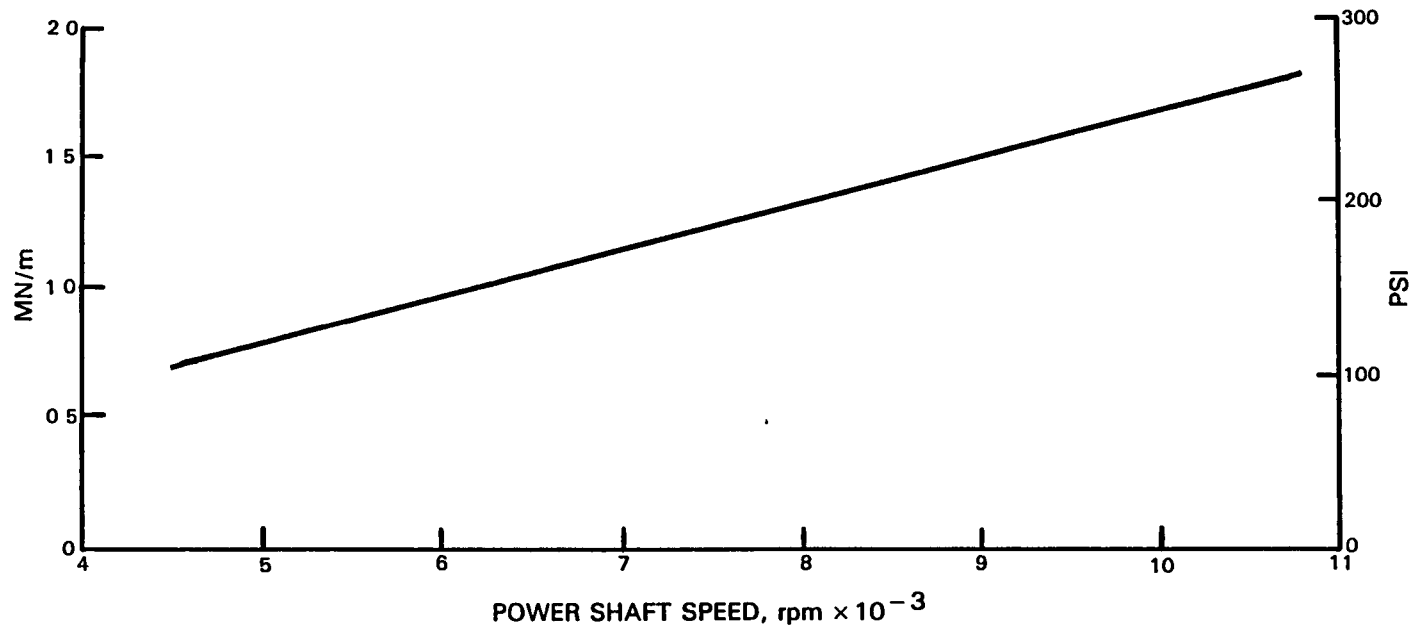
Figure 30   Conical Squeeze Film Available Supply Pressure
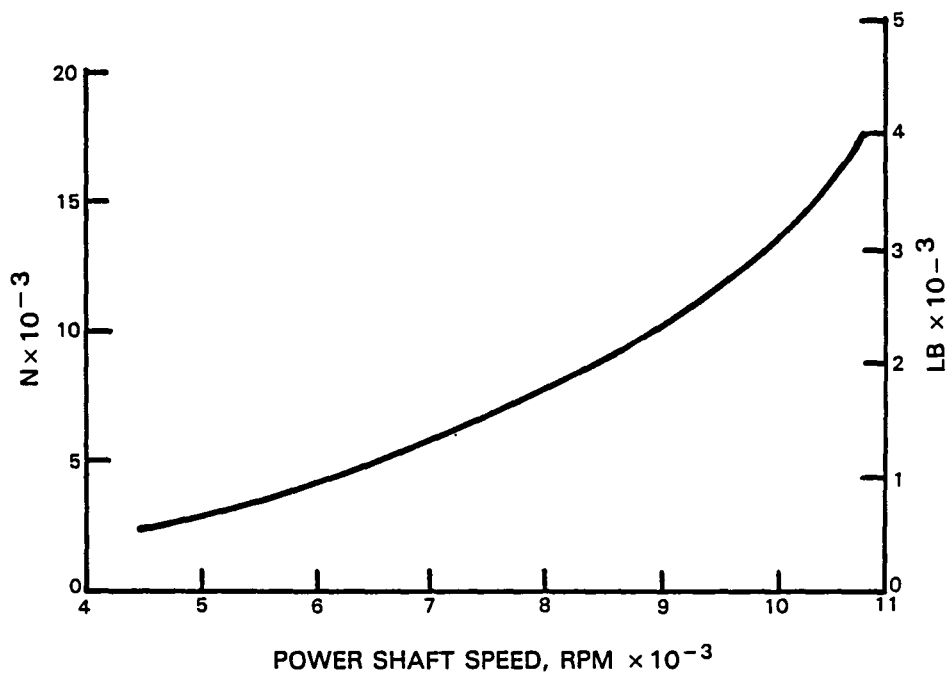
Figure 31   Axial Thrust Load Over Speed Range on Power Shaft Ball Bearing
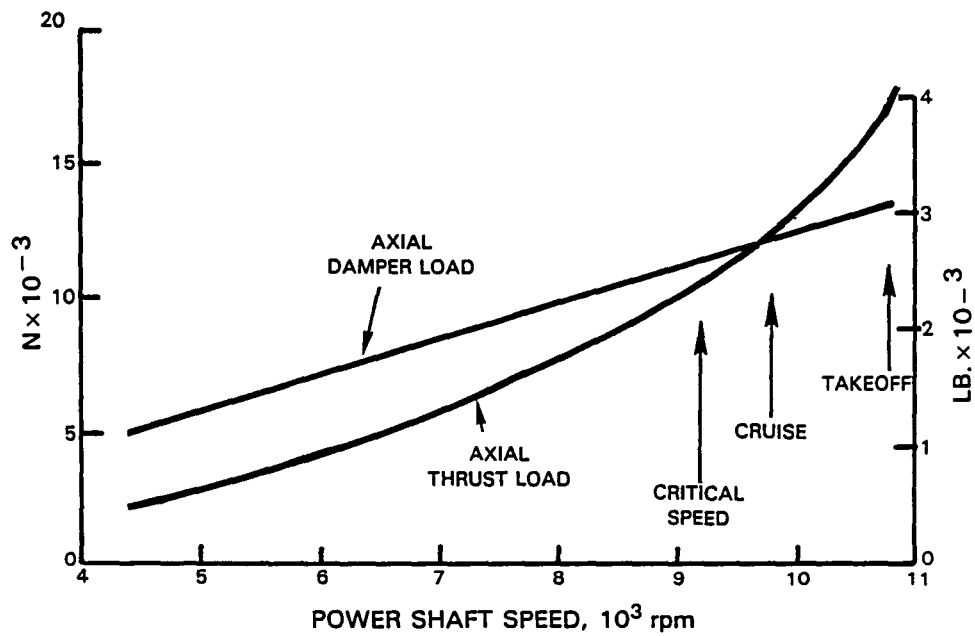

Figure 32   Relationship Between Thrust and Conical Squeeze Film Axial Loads
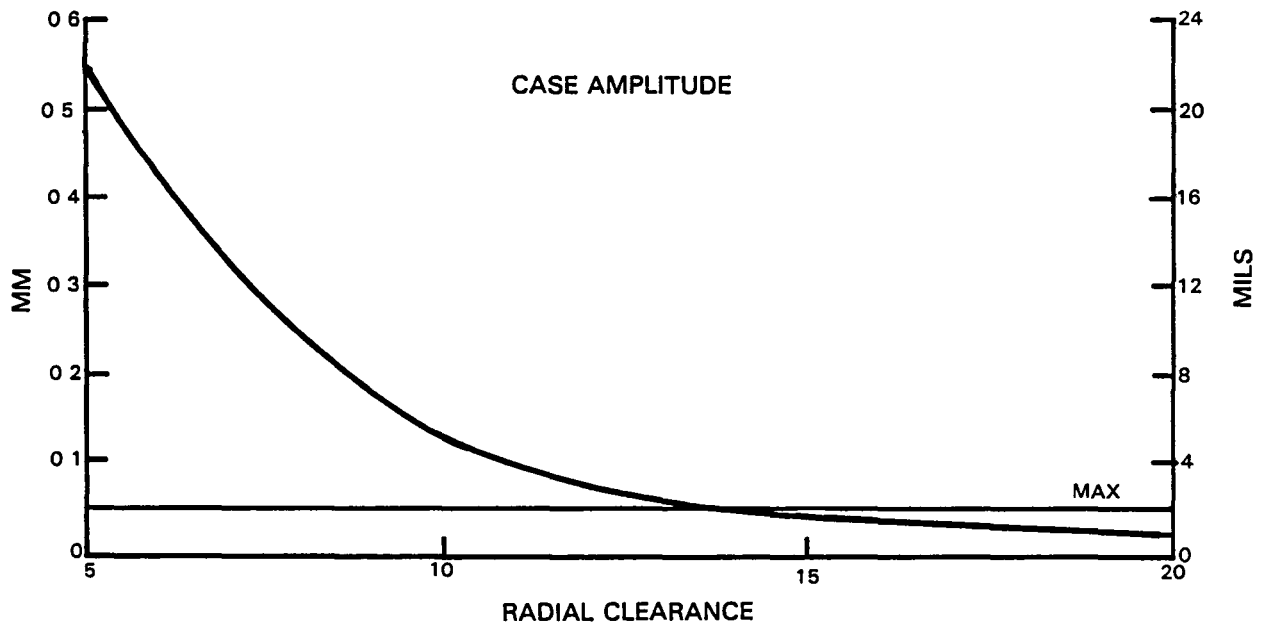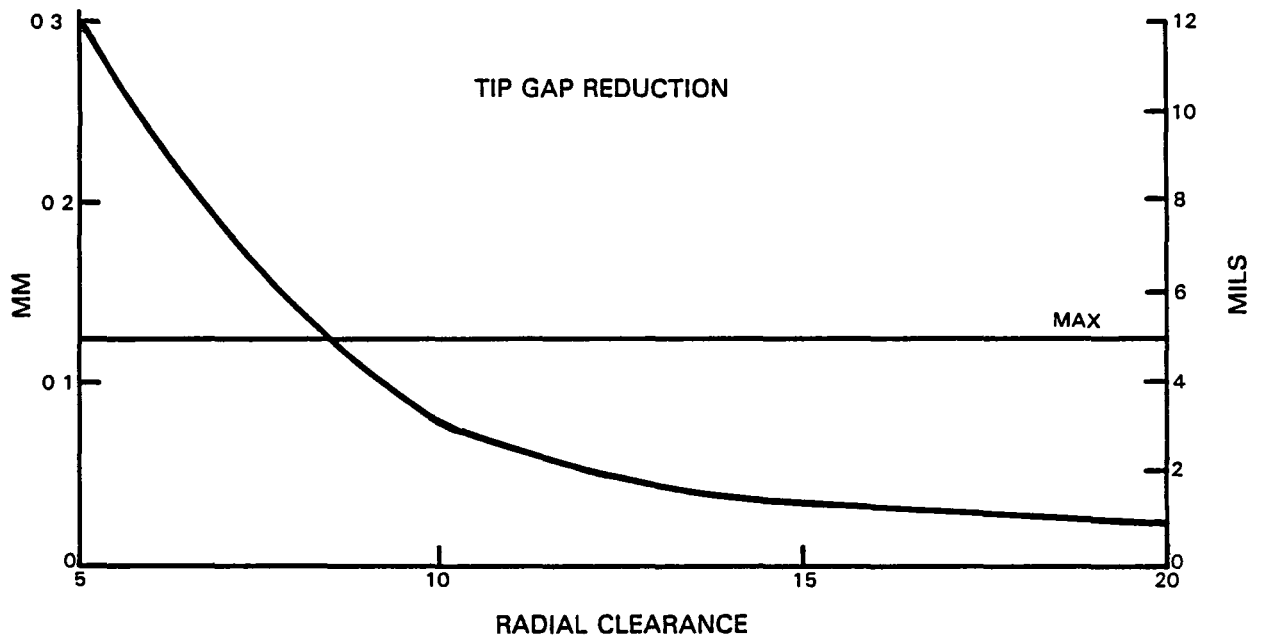
57

Figure 33 Effect of Varying Conical Squeeze Film Clearance on Gap Reduction
and Case Deflection Due to 2 oz-in. Power Shaft Unbalance
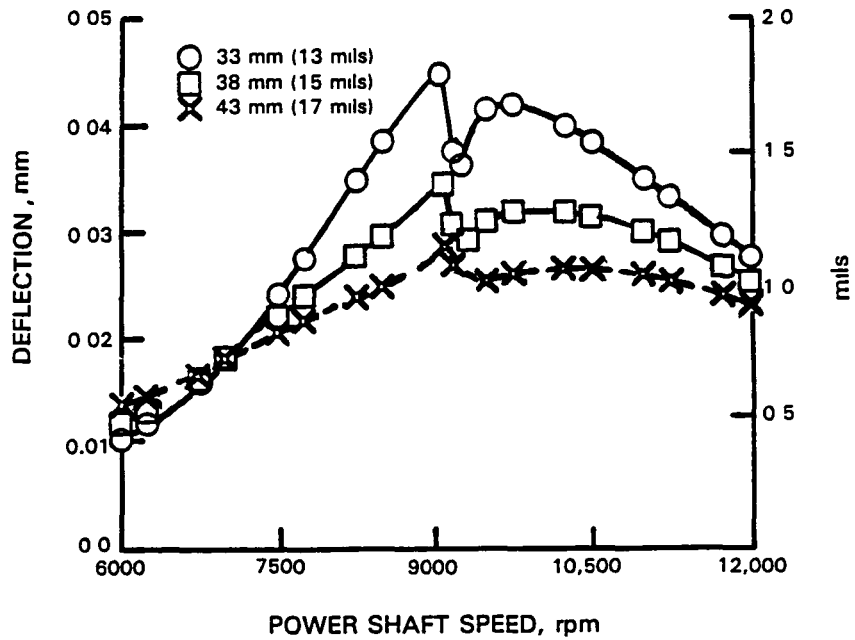
Figure 34   Effect of Varying Clearance of Conical Squeeze Film on Gap Reduction Due to 2 oz-in. Unbalance in Power Shaft
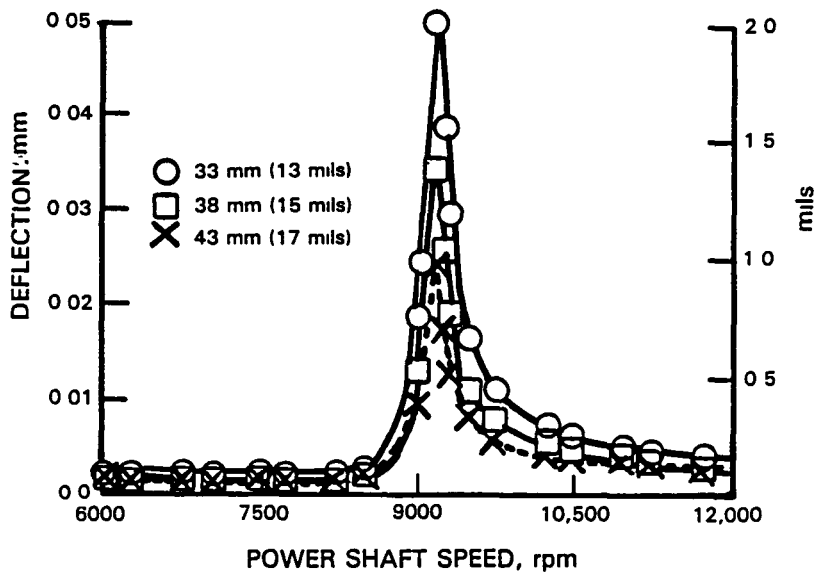

Figure 35   Effect of Varying Clearance of Conical Squeeze Film on Case Amplitude Due to 2 oz-in. Unbalance in Power Shaft

5.5.3.3 High Load Capability

A high imbalance load analysis with 2016 gm-cm (28 oz-in.) unbalance at the turbine, indicative of the loss of a turbine blade, was run. With reference to Table XI, it is seen that the damper is able to meet the required criteria. The numbers reflect a cavitated oil film damper since the uncavitated dynamic pressure of 2.4 MN/m^2 (350 psi) exceeded the available supply pressure of 1.7 MN/m^2 (243 psi).

Table XI

Conical Damper High Load Capability
2016 gm-cm (28 oz-in.) Imbalance

	Requirement	Predicted
Tip Gap Deflection	1.8 mm	1.1 mm
	(70 mil)	43 mil)
Bearing Load	66,700 N	31,600 N
	(15,000 lb)	(7,100 lb)

5.5.3.4 Summary

A conical squeeze film appears to be able to meet the required design goals with minimum requirements for new, untested technology. Concerns however include: liftoff behavior and orbit position; minimal trunnion capability of the damper making the inner ring susceptible to shaft slope as well as tilting due to pressure line of action not reacted through the inner ring center of gravity; rotor/engine reaction to 1E axial load due to rotor whirl; and supply pressure variance. It is concluded that the design is practical and worth experimental investigation. A key outcome of the concept is the ability to damp lateral/angular motion of the rotor as well as axial, thus enhancing the stability characteristics of the rotor.

SECTION 6.0

CONCLUSIONS AND RECOMMENDATIONS

The completion of the work reported herein has contributed to the development of viable lateral damping concepts for thrust bearings. The operational characteristics, relative advantages and disadvantages, and applicability of several concepts were thoroughly investigated. By basing the concept comparison on the use of weighting factors, the ranking resulted in the best concept for each engine class. Results of the concept evaluation and selected concept analytical investigation led to the following conclusions:

o   Relatively higher cost and weight and more difficult installation made the hybrid boost bearing, hydraulic thrust piston, and rolling element thrust face poorer candidates than the other concepts.

o   The curved beam, elastomer, and conical squeeze film damper designs are predicted to meet the required axial thrust requirements as well as dynamic stiffness and damping for their particular engine class.

o   The curved beam damper is the most reliable and predictable means to react axial thrust load, but size and weight restrictions limit the concept to larger engines.

o   In order to meet low cost and weight design requirements, the conical squeeze film damper should be designed with axial thrust face washers. The friction load on the washers is alleviated due to tne axial load carrying capability of the squeeze film.

o   Experimental data, used to define short-term elastomer behavior, are adequate to initialize a design. However, more durability testing with full damper compartment environmental effects is required in order to guarantee the predicted properties throughout the design life.

This study has resulted in a substantial increase in the understanding of the requirements for and means to accomplish lateral damping of thrust bearings. A follow-on experimental effort is justified in order to evaluate the validity and applicability of the three selected damper concepts: curved beam, elastomer, and conical squeeze film.

REFERENCES

1. Marmol, R. A., "Engine Rotor Dynamics, Synchronous and Nonsynchronous Whirl Control," Pratt & Whitney, Government Products Division, USARTL-TR-79-2, February, 1979.

2. Taylor, D. L. and V. S. Fehr, "Analysis and Design of Segmented Dampers for Rotor Dynamic Control," Journal of Lubrication Technology, Vol. 104, January, 1982, pp. 84-90.

3. Bhat, S. T., D. F. Buono and D. H. Hibner, "Analysis of High Load Dampers," NASA Report CR-165503, August, 1981.

4. Chiang, T., J. M. Tessarzik and R. H. Badgley, "Development of Procedures for Calculating Stiffness and Damping Properties of Elastomers in Engineering Applications, Part I: Verification of Basic Methods," NASA Report CR-120905, March, 1972.

5. Gupta, P. K., J. M. Tessarzik and L. Cziglenyi, "Development of Procedures for Calculating Stiffness and Damping Properties of Elastomers in Engineering Applications, Part II: Elastomer Characteristics at Constant Temperature," NASA Report CR-134704, April, 1974.

6. Smalley, A. J. and J. M. Tessarzik, "Development of Procedures for Calculating Stiffness and Damping Properties of Elastomers, Part III: The Effects of Temperature, Dissipation Level and Geometry," NASA Report CR-134939, November, 1979.

7. Darlow, M. S. and A. J. Smalley, "Development of Procedures for Calculating Stiffness and Damping Properties of Elastomers in Engineering Applications, Part IV: Testing of Elastomers Under a Rotating Load," NASA Report CR-135355, November, 1977.

8. Tecza, J. A., M. S. Darlow and A. J. Smalley, "Development of Procedures for Calculating Stiffness and Damping of Elastomers in Engineering Applications, Part V: Elastomer Performance Limits and the Design and Test of an Elastomer Damper," NASA Report CR-159552, February, 1979.

9. Reiger, A., G. Burgess and E. Zorzi, "Development of Procedures for Calculating Stiffness and Damping of Elastomers in Engineering Application, - Part VI," NASA Report CR-159838, April, 1980.

10. Rieger, A. and E. Zorzi, "Development of Procedures for Calculating Stiffness and Damping of Elastomers in Engineering Applications - Part VII," NASA Report CR-165138.

62

REFERENCES (continued)

11. Wilcock, D. F. and L. W. Winn, "The Hybrid Boost Bearing - A Method of Obtaining Long Life in Rolling Contact Bearing Applications," ASME Transactions, Journal of Lubrication Technology, Vol. 92, pp. 406-414, July, 1970.

12. Darlow, M. S. and E. Zorzi, "Mechanical Design Handbook for Elastomers," NASA Contract No. NAS3-21623, June, 1981.

13. Pinkus, V. and B. Sternlicht, "Theory of Hydrodynamic Lubrication," McGraw Hill, New York, N.Y., 1961.

14. Prohl, M. A., "A General Method for Calculating Critical Speeds of Flexible Rotors," Journal of Applied Mechanics, September, 1945.

15. Hibner, D. H., "Dynamic Response of Viscous Damped Multishaft Jet Engines," Journal of Aircraft, Vol. 12, Number 4, April, 1975.

16. U.S. Patent Number 4213661, July 22, 1980.

DISTRIBUTION LIST

LATERAL DAMPERS FOR THRUST BEARINGS
CONTRACT NAS3-23932

NASA-Lewis Research Center
21000 Brookpark Road
Cleveland, OH 44135
Attn: D. P. Fleming, MS 23-3
      (originals + 20 copies)

NASA-Lewis Research Center
21000 Brookpark Road
Cleveland, OH 44135
Attn: L. J. Kiraly, MS 23-3

NASA-Lewis Research Center
21000 Brookpark Road
Cleveland, OH 44135
Attn: R. L. Firestone, MS 500-305
      (2 copies)

NASA-Lewis Research Center
21000 Brookpark Road
Cleveland, OH 44135
Attn: Report Control Office, MS 60-1
      (2 copies)

NASA-Lewis Research Center
21000 Brookpark Road
Cleveland, OH 44135
Attn: J. Acurio, MS 302-2

NASA-Lewis Research Center
21000 Brookpark Road
Cleveland, OH 44135
Attn: G. J. Weden, MS 302-2

NASA-Lewis Research Center
21000 Brookpark Road
Cleveland, OH 44135
Attn: A. F. Kascak, MS 23-3

NASA Sci. & Tech. Info. Facility
P. O. Box 8757
Balt/Wash Internat'l Airport, MD 21240
Attn: Accessioning Dept.
      (25 copies)

NASA-Lewis Research Center
21000 Brookpark Road
Cleveland, OH 44135
Attn: J. S. Fordyce, MS 3-5

NASA-Lewis Research Center
21000 Brookpark Road
Cleveland, OH 44135
Attn: D. W. Drier, MS 86-2

NASA-Lewis Research Center
21000 Brookpark Road
Cleveland, OH 44135
Attn: Library, MS 60-3

NASA-Lewis Research Center
21000 Brookpark Road
Cleveland, OH 44135
Attn: Technology Utilization
          Office, MS 7-3

NASA-Lewis Research Center
21000 Brookpark Road
Cleveland, OH 44135
Attn: C. L. Walker, MS 302-2

NASA-Lewis Research Center
21000 Brookpark Road
Cleveland, OH 44135
Attn: L. D. Nichols, MS 49-6

NASA Ames Research Center
Moffett Field, CA 94035
Attn: Library

NASA Dryden Flight Res. Facility
P. O. Box 273
Edwards, CA 93523
Attn: Library

LATERAL DAMPERS FOR THRUST BEARINGS
CONTRACT NAS3-23932

NASA Goddard Space Flight Center
Greenbelt, MD 20771
Attn: Library

Jet Propulsion Laboratory
4800 Oak Grove Drive
Pasadena, CA 91103
Attn: Library

NASA Langley Research Center
Hampton, VA 23665
Attn: Library

NASA Johnson Space Center
Houston, TX 77058
Attn: Library

NASA Marshall Space Flight Center
Marshall Space Flt. Center, AL 35812
Attn: Library

NASA Marshall Space Flight Center
Marshall Space Flt. Center, AL 35812
Attn: ED 14/L. Schutzenhofer

NASA Headquarters
Washington, D.C. 20546
Attn: R/R. Colladay

NASA Headquarters
Washington, D.C. 20546
Attn: RT-6/C. Rosen

AVCO-Lycoming
550 S. Main Street
Stratford, CT 06497
Attn: E. Beardsley

AVCO-Lycoming
550 S. Main Street
Stratford, CT 06497
Attn: M. Saboe

AVCO-Lycoming
550 S. Main Street
Stratford, CT 06497
Attn: Library

Curtis-Wright Corp.
One Passaic Street
Woodridge, NJ 07075
Attn: Library

Franklin Inst. Res. Laboratories
20th and Parkway
Philadelphia, PA 19103
Attn: Library

Franklin Inst. Res. Laboratories
20th and Parkway
Philadelphia, PA 19103
Attn: Friction & Lub. Laboratory

Kaman Aerospace Corporation
Old Windsor Road
Bloomfield, CT 06002
Attn: Library

Mechanical Technology, Inc.
968 Albany-Shaker Road
Latham, NY 12110
Attn: Library

Mechanical Technology, Inc.
968 Albany-Shaker Road
Latham, NY 12110
Attn: E. S. Zorzt

Pratt & Whitney-FRDC
P. O. Box 2691
West Palm Beach, FL 33402
Attn: V. S. Fehr

Pratt & Whitney-FRDC
P. O. Box 2691
West Palm Beach, FL 33402
Attn: Library

Williams International
2280 W. Maple Road
Walled Lake, MI 48088
Attn: Library

LATERAL DAMPERS FOR THRUST BEARINGS
CONTRACT NAS3-23932

Air Force Aero Propulsion Laboratory
Wright Patterson AFB, OH 45433 ·
Attn: AFAPL/SFL/H. F. Jones

Air Force Aero Propulsion Laboratory
Wright Patterson AFB, OH 45433
Attn: AFWAL/POTC/L. Gill

Air Force Aero Propulsion Laboratory
Wright Patterson AFB, OH 45433
Attn: AFWAL/NASA-PO/E.E. Bailey

Aerojet-General Corporation
1100 W. Hollyvale
Azusa, CA 91702
Attn: Library

Aerospace Corporation
P. O. Box 90585
Los Angeles, CA 91745
Attn: Library

Garrett Turbine Engine Co.
111 S. 34th Street
Phoenix, AZ 85010
Attn: Library

Garrett Turbine Engine Co.
111 S. 34th Street
Phoenix, AZ 85010
Attn: T. Howell

AiResearch Manufacturing Company
9851 Sepulveda Blvd.
Los Angeles, CA 90009
Attn: Library

Battelle Columbus Labs
505 King Avenue
Columbus, OH 43201
Attn: Library

Boeing Company
Aerospace Division
P. O. Box 3707
Seattle, WA 98124
Attn: Library

Boeing Company
Vertol Division, Boeing Center
P. O. Box 16858
Philadelphia, PA 19142
Attn: Library

General Electric Company
Aircraft Engine Business Group
1000 Western Avenue
Lynn, MA 01910
Attn: R. A. Dangelmaier

General Electric Company
Aircraft Engine Business Group
1000 Western Avenue
Lynn, MA 01910
Attn: J. Paladino

General Electric Co.
Aircraft Engine Business Group
Cincinnati, OH 45215
Attn: A. F. Storace

General Electric Company
Building 55-219
Schenectady, NY 12345
Attn: E. R. Booser

General Electric Company
Mechanical Technology Laboratory
RD Center
Schenectady, NY 12301
Attn: Library

General Motors Corporation
Allison Division
Indianapolis, IN 46206
Attn: Library

Hughes Aircraft Corporation
Centinda and Teale Avenue
Culver City, CA 90230
Attn: Library

Lockheed Missiles & Space Company
P. O. Box 504
Sunnyvale, CA 94088
Attn: Library

Naval Air Systems Command
Washington, DC 20360
Attn: Library

Naval Air Propulsion Center
Trenton, NJ 08628
Attn: R. Valori

Office of Naval Research
Arlington, VA 22217
Attn: Library

U. S. Army Engineering R&D Labs
Gas Turbine Test Facility
Fort Belvoir, VA 22060
Attn: W. Crim

U. S. Army Research & Tech. Labs.
Fort Eustis, VA 23604
Attn: Library

U. S. Army (AVSCOM)
4300 Goodfellow Blvd.
St. Louis, MO 63120
Attn: E. J. Hollman, DRDAV-Q

General Motors Corporation
Allison Division
Indianapolis, IN 46206
Attn: W. H. Parker

Institute for Defense Analyses
400 Army-Navy Drive
Arlington, VA 22202
Attn: Library

National Science Foundation
Engineering Division
1800 "G" Street, NW
Washington, DC 20540
Attn: Library

Transamerica Delaval
853 Nottingham Way
Trenton, NJ 08638
Attn: E. A. Bulanowski

Rockwell International
Rocketdyne Division
6633 Canoga Avenue
Canoga Park, CA 91304
Attn: R. F. Beatty

Sundstrand Denver
2480 W. 70th Avenue
Denver, CO 80221
Attn: Library

United Technologies Corporation
Sikorsky Aircraft Division
Stratford, CT 06497
Attn: L. Burroughs

U. S. Army Research & Tech. Labs.
Fort Eustis, VA 23604
Attn: John White

U. S. Army (AVSCOM)
4300 Goodfellow Blvd.
St. Louis, MO 63120
Attn: J. T. Conroy, DRDAV-QE

LATERAL DAMPERS FOR THRUST BEARINGS
CONTRACT NAS3-23932

U. S. Army (AVSCOM)
4300 Goodfellow Blvd.
St. Louis, MO 63120
Attn: M. Raglin, DRDAV-QE

Southwest Research Institute
P. O. Box 28510
San Antonio, TX 78284
Attn: A. J. Smalley

Ingersoll-Rand Corporation
Phillipburg, NJ 08865
Attn: R. G. Kirk

University of Virginia
School of Eng. & Applied Science
Charlottesville, VA 22901
Attn: Dr. Paul Allaire

Texas A&M University
Dept. of Mechanical Engineering
College Station, TX 77843
Attn: Dr. J. M. Vance

Case-Western Reserve University
Dept. of Mechanical Engineering
Cleveland, OH 44106
Attn: M. L. Adams

Army Research Office
P. O. Box 12211
Research Triangle Park, NC 27709

Southwest Research Institute
P. O. Box 28510
San Antonio, TX 78284
Attn: Library

Teledyne CAE
1330 Laskey Road
Toledo, OH 43612
Attn: R. H. Gaylord

University of Virginia
School of Eng. & Applied Science
Charlottesville, VA 22901
Attn: Dr. Edgar J. Gunter

The Vibration Institute
101 W. 55th Street, Suite 206
Clarendon Hills, IL 60514
Attn: Dr. R. L. Eshleman

Texas A&M University
Dept. of Mechanical Engineering
College Station, TX 77843
Attn: Dr. D. W. Childs

Cornell University
Dept. of Mechanical Engineering
Ithaca, NY 14853
Attn: D. L. Taylor

Mr. Art Leiser, P&W Rep.
24500 Center Ridge Road, Suite 280
Westlake, OH 44145

68

DISTRIBUTION LIST (continued)

LATERAL DAMPERS FOR THRUST BEARINGS
CONTRACT NAS3-23932

INTERNAL DISTRIBUTION

D. H. Hibner
MS 163-09

P. Brown
MS 163-07

H. Lemasters
MS 163-09

S. Fletcher
MS 118-35

H. Kocar
EII System Files
MS 118-19

D. R. Szafir
MS 163-09

Library
MS 129-01

C. Lenkeit
MS 162-30

D. Avery
MS 118-35

I. Goldberg, AFPRO
MS 104-08 (letter only)

End of Document